# Reply to Referee #2 follows Reply to Referee #1 A marked document follows Reply to Referee #2 Green = Changes for Referee #1 Grey for referee #2

Comments on NO2 and HCHO measurements in Moore's from 2012 to 2016 from Pandora spectrometer instruments compared with OMI retrieval and with aircraft measurements during the Korus-AQ campaign by Jay Herman et al.

General comments.

This paper is about observations of tropospheric columns of HCHO and NO2 in 8 sites located in Korea, by using a Ground Based-direct Sun spectrometric instrument prior and during a study about Air Quality called KORUS-AQ. Observations have a different temporal extension depending on the site and varies from 1 to 5 years.

Comparisons to NO2 OMI-Aura OMNO2 V03 and to measurements made by using the CAMS instrument on board of an aircraft are also presented in this work.

Ground based (GB) data are very valuable and interesting and this paper states the importance of GB measurements in comparison to satellite measurements available at the moment of the campaign that cannot capture the diurnal variation of pollution, necessary to state the Air Quality. It is also very valuable the effort devoted to keep operative 9 different instruments during one to five years.

In my opinion the work is very descriptive with a lack of interpretation of the measurements, instead, this article is in the scope of AMT journal and it should be published after taking into account some specific comments and technical corrections.

Specific comments.

Please note: the colors used – Green for changes to the paper; Yellow for my comments in reply to your review; No color for your review text

Introduction.

It would be clarifying if a brief introduction of the campaign, why in Korea, objectives, and kind of instrumentation or citation of other works done during this campaign (if it is the case) would be included in the introduction. Also why the target gases to be measured are HCHO and NO2. Previous works in AQ in Asian megacities (i.e., using MAXDOAS technique) should be also mentioned in the introduction to put these measurements in context.

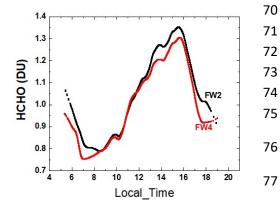
### The introduction now reads

The purpose of this paper is to present the retrieved amounts of nitrogen dioxide and formaldehyde, NO<sub>2</sub> and HCHO, obtained from Pandora Spectrometer instruments (PSI) during the KORUS-AQ campaign (Korea US Air Quality: May – June 2016). Quoting from a NASA website: "Korea U.S.-Air Quality (KORUS-AQ) is a joint field study between NASA and the Republic of Korea to advance the ability to monitor air pollution from space. The campaign will assess air quality across urban, rural and coastal South Korea using observations from aircraft, ground sites, ships and satellites to test air

quality models and remote sensing methods. Findings will help develop observing systems using models and data to improve air quality assessments for decision makers." A thorough description of the KORUS-AQ campaign and its motivations is given in a pre-campaign white paper, <a href="https://espo.nasa.gov/korus-aq/content/KORUS-AQ">https://espo.nasa.gov/korus-aq/content/KORUS-AQ</a> White Paper.

Assessing air quality in South Korea is of interest because of the levels of pollution arising from high densities of population and intense industrial activity associated with the production of  $NO_2$ . Recent measurements of surface concentrations of  $NO_2$  and comparisons with satellite data demonstrate the need for high quality ground-based measurements to augment satellite observations (Kim et al., 2017; Jung et al., 2017). The driving reason behind the interest is the effect of elevated levels of  $NO_2$  in Korea on human health (Kim and Song, 2017 and references therein). Measurements of  $NO_2$  from aircraft have been used to obtain altitude profiles to compare with data obtained from fixed site measurements and to obtain a national scale estimate of pollutant exposure (Lee et al., 2015; Kim and Song, 2017).

In addition to NO<sub>2</sub>, PSI measurements were used to assess the amount of Formaldehyde (HCHO) present in the air. This is important because of HCHO potential impact on health (Zhang et al., 2013, ) and because it plays a strong role in tropospheric reactions leading to the formation of boundary layer ozone. Sources of HCHO are from atmospheric reactions with volatile organic compounds (VOC) emitted from ground sources and industrial activities (Lee at al., 2009). A previous paper describes HCHO retrievals from a PSI located at Yonsei University in Seoul using a similar spectral fitting retrieval algorithm used in the current study (Park et al., 2018), but using a different wavelength fitting range, 335 – 358 nm instead of 332 – 359 nm used in this study. The choice of spectral fitting window is discussed in Spinei et al. (2018).



To give an idea of the effect of different fitting windows, I am showing a graph to the left. This paper used fitting window 4 (FW2 332 – 359 nm). For NO<sub>2</sub>, there is no ambiguity with fitting window. For HCHO, the ambiguity comes from cross-correlation effects with O3, NO<sub>2</sub>, and BrO. FW2 is 324-360 nm

Some information about the different instruments, technique and retrieval of data should be included in this work:

The instruments described in this paper are Pandora, details given in this paper, OMI satellite instrument, 4-STAR, described in this paper, and CAMS.

Added Line 463: Quoting from Richter et al., 2015, "CAMS is a multi-species spectrometer configured for the simultaneous detection of ethane (C2H6) and formaldehyde (CH2O). The spectrometer utilizes a tunable, fiber optically pumped difference frequency generation laser source in combination with a Herriott type multi-pass absorption cell with an effective path length of 89.6 m"

89 90 91

92

86 87

88

Line 318: OMI is a polar orbiting push broom hyperspectral instrument (300 – 500 nm with resolution of 0.45 nm in the UV and 1 nm in the visible and a spatial resolution of 13 x 24 km<sup>2</sup>) onboard the AURA satellite

93 94 95

I suppose that Pandora retrieval is based in a DOAS algorithm, but if not, the kind of algorithm used should be, at least, mentioned and cited. If it is the case, a small mention to DOAS retrieval or DOAS technique should be included in the text and cited.

97 98 99

100

101

96

The retrieval technique and error estimates for HCHO are discussed in a companion paper, Spinei et al. (2018) also submitted to AMT. The PSI description is given starting on Page 4 and in included references. The algorithm is a modified form of DOAS. The big difference is that there is no attempt to flatten the spectral shape (important for ozone), but not for NO<sub>2</sub> or HCHO.

102 103 104

105

Regarding to OMI, characteristic of the data used would be welcome in order to sustain some statements about the differences between GB and satellite measurements mentioned along the text. I will revisit this point later on in the proper section.

106 107 108

109

110

For the interpretation of CNO2, it would be interesting to mention what is the contribution to CNO2 of stratospheric column, if stratospheric and tropospheric contribution can separated and what is the sensitivity to troposphere of Pandora instrument.

111 112 113

114

For polluted regions, such as Seoul or Olympic Park, the stratospheric amount of NO2 (0.1±0.05 DU) is negligible compared to the total column amount 0.5 to 3 DU. The stratospheric column cannot be separated, but is small compared to the tropospheric amount.

115 116 117

On Page 4 I have added

118 Figures 3 and 4 summarize all of the Pandora C(NO<sub>2</sub>) data obtained during the KORUS-AQ 119 campaign. Figure 3 presents histograms in percent frequency of occurrence for all nine sites. All of the 120 sites located within or downwind of major cities have production of NOx mainly from transportation and 121 power generation as its major sources. The ratio of transportation NOx production compared to all other sources is estimated as up to a factor of three (Kim et al., 2013). Of these sites, Anmyeondo 122 123

frequently (40%) retrieves values of C(NO2) that are close to the typical stratospheric values of 0.1±0.05

DU. Other sites occasionally have clean days with similar low values.

124 125 126

127

NO2 during KORUS-AQ campaign.

128 129 130

131

132

For the interpretation of CNO2, it would be interesting to mention what is the contribution to CNO2 of stratospheric column and for AQ purposes to what extent tropospheric column resides below boundary layer. Also would be important to state what the sensitivity to troposphere of

133 Pandora instrument is.

The sensitivity to stratospheric and tropospheric  $NO_2$  are approximately the same as long as direct-sun measurements are possible. The estimated retrieval error is  $\pm 0.05$  DU with a precision of  $\pm 0.01$  DU. This has been mentioned on Page 5 line 147. Figure 4 demonstrates this accuracy and precision.

Later on, in this same section you consider that measured CNO2 at Anmyeondo is mainly stratospheric. How can you differentiate this stratospheric contribution? See above

In order to have a reference, which level of CNO2 is typical of polluted places? In the US, a value of 0.3 DU would be typical In Korea a value of 0.5 DU is common.

Line 173: I added, "Typical C(NO<sub>2</sub>) amounts are 0.3 to 0.5 DU in polluted regions."

A previous intercomparison of two of the GB instruments used in this work has been done with a very good agreement. But, to what extent is this good agreement extensive to the remaining GB instruments?

Of the new instruments installed during KORUS-AQ (not the older instruments Seoul and Busan), they were run side by side at Goddard Space Flight Center with similar results. Our experience is that shipping does not alter the calibration.

From figure 2a, lower panel, it seem that there is a level of cloud or aerosol coverage that limits the agreement between the two GB compared instruments. It can be seen that between 17 and 18h where the difference between instruments is greater than 0.05 DU. Has been carried out any study in which this level has been delimited in order to exclude these data for this work? Or this situation only is observed when high coverage (due to cloud or aerosol) and low CNO2 are coincident? Is this situation contemplated by applying the filter of CNO2 error >0.1 DU?

All data with error estimates > 0.1 DU were eliminated. The purpose of Figure 2 is to demonstrate that good retrievals do not require perfectly clear skies.

In page 8, L185, it is said that figure 3 and 4 are consistent with a large NO2 pollution source in the Seoul metropolitan area that tends to transport eastward to the eastern stations near Seoul. This is not totally clear for me since there must be sources in all the cities, as traffic. It is also difficult to see from the different axis for different stations in figure 3. Please, explain this point with more detail. In figure 4 it is difficult to see.

The highest pollution sources are close to the Seoul metropolitan area. This includes Olympic Park just to the east of Seoul. As one proceeds eastward from Seoul to Taewha, the traffic level and population density diminishes from extremely heavy to moderate. All of the sites have their own local sources augmented by transport. Since I do not model the transport of NO2, I have removed the speculation about transport.

The sentence now reads, ". Figures 3 and 4 show that sites near Seoul metropolitan area (Olympic Park) have larger amounts of pollution compared to those further away (Taehwa, Songchon, and Yeoju)."

180 In line 189, are you referring figure 4 instead figure 5?

It should be (Figs. 4 and 5)

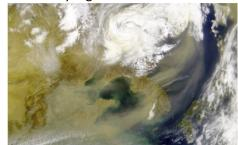
Busan is located in the eastern coast, maybe NO2 is transported from Busan to the Ocean but attending to the eastward transport proposed for Seoul and eastern stations surrounding Seoul, the amounts of NO2 in Busan shouldn't be given by transport from western locations? But considering that the mechanism of transport to the Ocean is the cause for CNO2 dissipation in Busan, why are there some days that this mechanism doesn't work and concentrations over 3 DU are observed? Just in case, this situation is observed only 3 days. Is there any common pattern for them?

NO2 from Busan certainly reaches the ocean areas just to the east of the city and probably dilutes the total amount over the city. I changed the sentence to read <u>some</u> in place of <u>much</u>, "Busan is located on the southeastern coastline, so that some of its  $NO_2$  pollution dissipates over the ocean, except for occasional days when very high amounts (3 DU) occur.

Busan, while smaller than Seoul, has a very high density of people located near the city center and quite heavy traffic. On days when there is little wind, NO2 will accumulate in the lower troposphere.

Occasional plumes observed at Anmyeondo, are supposed to come from Northwards or China, is there any evidence of this? Maybe a retro trajectory for these days? Literature?

Satellite pictures showing dust transport are common. These also carry NO2 when the wind levels are reasonably high.



I changed the sentence to be more speculative, since I have no direct evidence of the source. The island region Anmyeondo during the KORUS-AQ campaign had little traffic and a low population density.

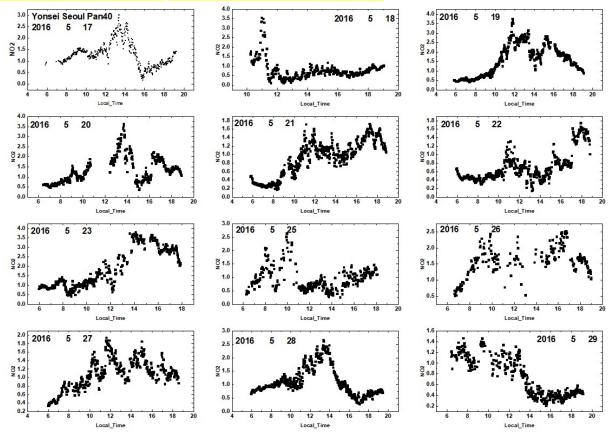
"The most frequently occurring  $C(NO_2)$  value at Anmyeondo is 0.15 - 0.2 DU, which means that the measured  $NO_2$  amount are <u>partly</u> from the stratosphere with very little tropospheric or boundary layer  $NO_2$ . There are occasional  $C(NO_2)$  plumes that <u>could</u> be from industrial activity to the north, and, perhaps, from China. Transport of  $NO_2$  from China occurs episodically in significant amounts (Lee et al., 2014)."

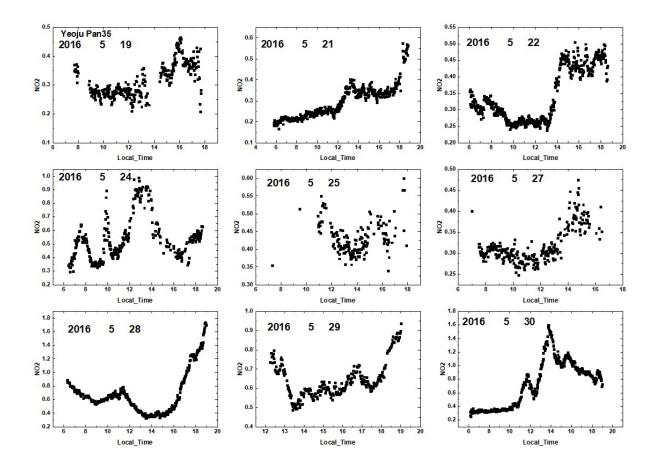
Diurnal variation of CNO2

Is there any explanation for the increasing of CNO2 at the late afternoon? The high amounts of CNO2 observed at Seoul even in the morning are associated with an anticyclonic situation when high pressures confine pollutants in the boundary layer? Or it is always the same, no matter the meteorological situation is? The evolution from days 130 to 150 could indicate an anticyclonic situation followed by a low pressure system (rain or wind) because the following days seems to

be less polluted. This meteorological situation could also explain the increase along the day of CNO2. Regarding the eastern stations around Seoul, they have not only the transported air masses from Seoul but also their own sources. This is not easy to interpret without a chemical model but do you think it could explained the two maxima observed at midday and at late afternoon at Olympic Park and Taehwa Mt? It is a pity that the series for these last stations stops at day 150, maybe the same behavior than at Seoul could be observed.

The weather during the KORUS-AQ days was frequently partly cloudy with some days of rain. Not the best measuring weather. However, I do not know what the wind conditions were relative to the rooftop of the physics building at Yonsei. The building is substantially elevated over the main city streets. I am showing here a series of individual plots for 12 days for Seoul and 9 days for Yeoju. The patterns are not clear. Most of the time, the amount increases in the afternoon, but there are morning peaks (25<sup>th</sup>). I have also included some daily plots from Yeoju. The pattern is irregular. The 3-D plots give the general idea of the diurnal variation. The plots below are not in the paper





Could you cite instead the source for automobile emission from which the brochure of Thermo

Sci is taken? I cannot find a journal reference to the measurements made by the company. However, I added a reference related to NO/NO2 ratios (Walters et al., 2015)

To compare to Boersma et al. and extract any conclusion it would be necessary to know if the meteorological situation considered in Boersma et al., is the same than in this work. Is it the same? This is not clear enough in the text. The situation observed by Boersma et al. is in the same kind of environment? I removed the reference to Boersma et al.

Longer-term changes in CNO2

Figure 6 and text would be gain in clarity if L(t), M(t) and ZM(t) would be identified in the figure 6

ZM(t) and L(t) are not shown in Figure 6. As it says in the text, The "zero slope functions" are obtained by subtracting a linear least squares fit L(t) to monthly running average curves M(t) in panels C and F to form zero slope functions ZM(t) = M(t) - L(t)." However, M(t) is shown in panels C and F. I have not labelled panels C and F.

It is difficult to see any monthly variation in the black line of panels B and E in that scale. Please,

change the scale from 0 to 1.5.

 There is almost no monthly variation in the deseasonalized time series. I am attaching two plots with the original and with an expanded inset scale for Gwangju. The first is the original  $NO_2$  data monthly running average. The second is the same plot after removing the seasonal behavior. These plots are now in an appendix.

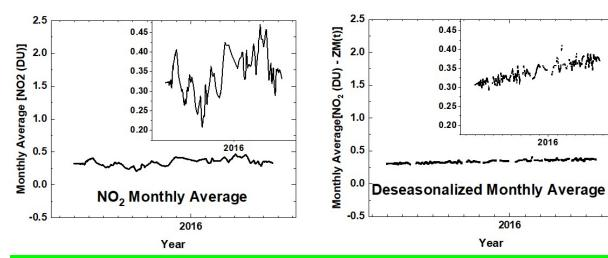


Fig. A1 An illustration of the deseasonalization (right panel) of the monthly running average of  $NO_2$  for the Gwangju site (left panel) shown in Fig. 6. The insets are magnifications of the main plots.

Less polluted stations, Gwangju and Anmyeondo show a positive trend in CNO2 whereas the remaining stations that are more polluted show a negative CNO2 trend. This is difficult to understand. Could you explain it a little?

For Gwangju and Anmyeondo, the time series are too short (13 Months) to infer that the changes represent increasing or decreasing long-term changes in pollution levels. The data from the two long term sites (Seoul and Busan) does suggest that clean-up efforts have occurred in spite of increasing population during the period of observation. Automobile exhaust has cleaned up considerably based on US data. I do not have access to Korean automobile exhaust data.

Short time series are a universal problem with acquiring "campaign" data instead of locating instruments permanently at fixed sites. The Pandora program is now implementing the long-term site approach. It is possible that Korean efforts at lowering pollution in larger cities are having an effect, but this data series is too short to support the hypothesis.

Comparison with OMI satellite Overpass Data.

Differences observed between OMI and GB instruments are surely due to the different observed air masses by OMI and GB, part of it would be due to the OMI FOV as it is stated in the text. In fact a better coincidence observed in Gwangju support this fact. This could be stated in the text since if differences are only due to OMI FOV, comparison would be more coincident in western stations.

To discuss this point a brief description of how have OMI data been calculated is important to

include. OMI overpass is only one point per day. But how has this point been calculated? By using the closest orbit to the station, as a averaging of some measurements? In this case a plot where the different points used by a OMI overpass could support the FOV as a cause of the observed differences. Small discussion about sensitivity of OMI to lower tropospheric NO2 and a discussion comparing it to Pandora sensitivity in troposphere or boundary layer is missed out in the text as well.

But the differences are also due to the hour of the overpassing. It is not possible for OMI to capture the elevated CNO2 observed at late afternoon, but you can check if the comparison improves when you don't consider late afternoon GB data.

The OMI data are acquired from the station overpass time series up to a maximum of 3 points per day (90 minutes apart), but usually 1 point per day. The distance from the central location does vary. The Pandora data are selected to be within 8 minutes of the overpass time, that is, up to an average of 16 Pandora points per OMI point. This is stated clearly in the opening paragraph of section 5. The OMI overpass data link is given in the paragraph. The data link contains the distance from the target site for every point in the time series. The overpass data does have varying distances. For most of the overpass data, the average distance is 20±20 km with a few points further away.

The 0-40 km variation plus the OMI field of view, which is quite large,  $13 \times 24$  km<sup>2</sup>, compared to city center dimensions. The result is that there is spatial averaging that reduces the high levels of  $NO^2$  seen in PSI measurements near the center of a highly polluted metropolitan area. For cleaner sites, the averaging does not produce as large an effect. Other OMI retrieval effects, such as uncertainty in the surface reflectivity and the size of the averaging kernel near the surface (sensitivity), produce errors that are much smaller than the differences seen against PSI.

Figure 9b is difficult to see. As you are using 3 month average data, it would be useful to see line+symbol instead only line. In that case it would be possible to see if there is not a displacement of minima, it is not clear for me if they are coincident.

The data are 3 month running averages. There are approximately 1500 data points. I have added a comment to the figure caption about running averages. There is no displacement of the minima

The data are derived from 3- month running averages of the daily data. Interpolation has been used where there are missing data points.

Please make minor grid lines darker for this figure and enlarge the plot in order that details can be seen. Done

Figure 9b shows the 1500 data points that are approximately a 3-month running average and the interpolation for missing data. These are just the solid curves in Figure 9b on an expanded scale.

It is very interesting that seasonal evolution is captured by OMI and GB the first two years in both stations and in the last two years for Seoul. But there is a double maxima in spring captured by GB in 2013 and 2014. Although it is not exactly in the scope of this paper, is there any explanation for this apparently unusual seasonal behaviour, especially for year 2014?

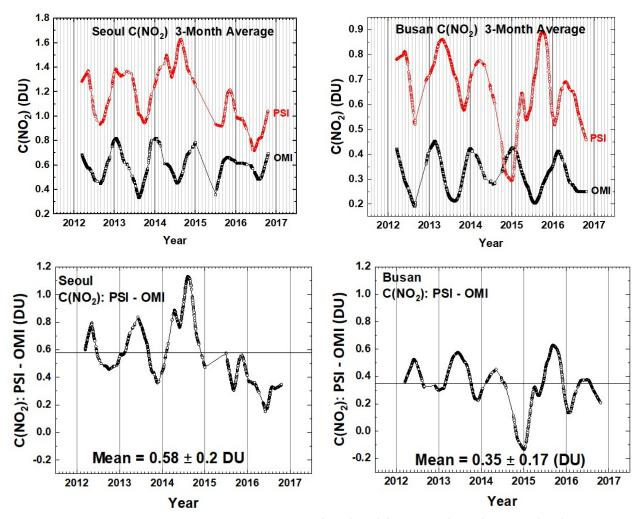


Fig. 9b Comparisons between the seasonal averages for  $C(NO_2)$  from OMI (black) and PSI (red) at Seoul and Busan for a 5-year period. The lower panels show the seasonal difference between the PSI and OMI. The individual data points are shown derived from a Lowess(0.1) smoothing, approximately a 3-month running averages of the daily data. Interpolation has been used where there are missing data points.

The minimum in CNO2 observed by GB in Busan at the end of 2014 is really surprising, is there any explanation for such behaviour?

This could be a local effect during winter months at the university in Busan. The PSI appears to have been operating normally. There is no periodic maintenance or recalibration of the PSI.

I don't think that the objective of OMI were to stated AQ in big cities, it is clear that continuous monitoring is a better technique to know the evolution of pollutants along the day in order to control the impact of pollutants on public health.

I agree. Polar orbiting satellites only give a midday snapshot of the pollution levels.

I have added: "The results from PSI suggest that local ground-based monitoring of pollution is important for estimating their impact on human health, particularly since amounts of C(NO<sub>2</sub>) occurring later in the afternoon exceed the amounts at the time of the satellite overpass."

Formaldehyde from five Korus-AQ sites

I don't know if this is even possible, but in order to investigate differences observed in CHCHO from PSI and aircraft instrument, it would be interesting to have both instrument measuring together a couple of days from GB in the same location. In this way it would be possible to estimate whether the differences are due to different retrieval or observation technique more than to the approximations made to correct the observed column from aircraft to compare to GB instrument.

The aircraft did operate on more than 1 day. I picked a sample from May and June to show typical results. Measurements from other days were very similar.

In figure 18, most of plotted days don't show the expected diurnal evolution, but an increase of HCHO along the day with greater amount observed at late afternoon, is there any explanation about this? The same behaviour is observed in figure 19a for the same station, it seems to be the habitual diurnal variation of HCHO for this site.

I'm not sure what the "expected" diurnal variation should be. Not enough measurements have been made to date.

Technical corrections.

Page 5, L 136. 2.0 should be 2 OK

Figure 2 has been changed to

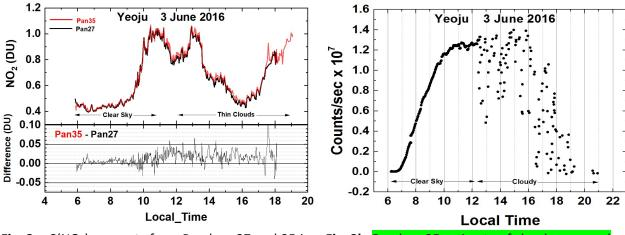


Fig. 2a C(NO<sub>2</sub>) amounts from Pandora 27 and 35 in Fig. 2b Pandora 35 estimate of cloud or aerosol

Yeoju, Korea during 3 June 2016 and their cover from measured counts/second at difference | Pan35 – Pan27 | < 0.05 DU. approximately 500 nm. 385 Figure 2a. Please include a grid in the lower panel that permits to see the level of ±0.05 DU. 386 OK 387 Figure 2a. Please remove last sentence of the caption. OK 388 389 Figure 2b. Please do not include an explanation in the caption but in the text. OK 390 The text now reads: "Figure 2b shows the effect of thin clouds in terms of reduced measured count rates 391 392 for a single spectrometer pixel near 500 nm showing a near noon count rate of  $1.26 \times 10^7$  counts/second 393 followed by a reduced count rate as clouds move in front of the sun. The cloud plus aerosol cover 394 estimate is from the same date 3 June 2016 as the C(NO<sub>2</sub>) amounts shown in Fig.2a." 395 396 397 Page 10 line 237 4.0 should be 4 OK 398 399 Figure 6. Dots are extremely difficult to see, please make them darker. Missing labels in x axis of 400 panel A, B and E. I tried making them darker. Except for a few high-value points, it makes no difference 401 in being able to see the individual dots. There are 5400 dots, most of which are near the black curve. There are no missing axis labels. Instead, panels A, B, D, and E have the same labels and same scale 402 403 (Years) broken down by Month. 404 405 Figure 6. Please explain in the caption what is the dark line in panel B and E. Re-organize the text 406 in the caption, it is very confusing. OK 407 408 The figure 6 caption is now: "Approximately 1 year of daily column C(NO<sub>2</sub>) amount data (Panels A and D) and the monthly running average amount (dark plot in Pandels A and D). The data are from GIST at 409 410 Gwangju and Amnyeondo. Panels A and D are the original time series with one data point every 80 411 seconds, panels B and E are the deseasonalized time series. Panels C and F are an expanded scale of the 412 monthly running averages M(t) of C(NO₂) that are identical to the solid lines in panels A and D. The 413 vertical extent (panels A, B, D, and E) on a given day is the range of diurnal variation from early morning 414 to late afternoon" 415 416 Also, see the graphs near line 247 of this reply. The insets show the results of deseasonalization. 417 418 Figure 6. Greater plots and vertical grid would be also very useful. I added the vertical grid 419 420 Figures 17 and 18. Please include vertical grids. Put greater tick labels. OK 421 422 Figures 19a and 19b, please darken the dot, they are difficult to see. Add vertical grids to the left

panels. There are over 11000 points for each site. Darkening the points will not make them visible

423

424

425 426 except for outliers.

Figure 19b panel B, correct typo for Anmyeondo OK

Please note the color coding. Green was for Referee 1 and Gray for referee 2. I used **bold** for replies to referee 2 that are not inserted into the paper.

Interactive comment on " $NO_2$  and HCHO measurements in Korea from 2012 to 2016 from Pandora Spectrometer Instruments compared with OMI retrievals and with aircraft measurements during the KORUS-AQ campaign" by Jay Herman et al.

Anonymous Referee #2 Received and published: 10 June 2018

### **General comments:**

The manuscript entitled " $NO_2$  and HCHO measurements in Korea from 2012 to 2016 from Pandora Spectrometer Instruments compared with OMI retrievals and with aircraft measurements during the KORUS-AQ campaign" presents total vertical column measurements of NO2 and HCHO with 9 Pandora instruments at 8 sites during a field campaign in Korea in 2016 (May-June) and from 1 to 5 years before, depending on the station. An investigation of the pollution levels at the 8 different sites, the diurnal pattern of  $NO_2$  and HCHO as well as NO2 long-term trends are presented.

During the campaign, additional measurements of the  $NO_2$  column using the 4STAR airborne sun photometer and of the altitude profile of HCHO using the air-borne CAMS instrument have been performed, which are compared to the columns measured by the ground-based Pandora instruments. On a longer time series of 1 and 5 years, respectively, a comparison to OMI  $NO_2$  satellite measurements is presented. At last, the Pandora HCHO measurements during the campaign are compared to HCHO measurements from OMI.

The paper highlights nicely the importance and advantages of ground-based measurements with a high temporal resolution for the investigation of local, surface near air pollution in comparison to satellite measurements, which cannot capture the diurnal cycle and tend to underestimate local pollution hotspots due to the large averaging area of the ground pixels.

The paper is well structured and the scientific approach is clearly described. However, the objective and aim of the campaign should be declared more clearly in the text and in some cases the interpretation of the results is lacking.

All in all,I believe this paper is in the scope of AMT and should be published, with some minor improvements, based on answering my specific comments below:

## **Specific comments:**

Abstract, line 44: What kind of average is meant by the mentioned "PSI C(NO2) averages" and "OMI averages"?

PSI C(NO<sub>2</sub>) 30-day running averages

Introduction: Please mention that these are direct sun measurements.

**I added**: "The intent of the network was to integrate direct-sun column density observations of NO<sub>2</sub> and HCHO into a multi-perspective framework of observations including ground-based, satellite, and airborne measurements of air quality."

The objective and aim of the campaign should be declared more clearly in the text. Done

Although the cited reference Spinei et al., 2018 discusses the analysis procedure very extensively, please mention in the introduction at least briefly the retrieval algorithm (DOAS?), what kind of reference spectrum is used and how the measured slant columns from the direct sun measurements are converted into vertical columns.

The following has been added

"The retrieval algorithm is based a direct-sun spectral fitting method similar to the wellaccepted DOAS (Differential Optical Absorption Spectroscopy, Platt, et al., 1979 and Platt, 1994 ). NO2 absorption cross sections were obtained from the laboratory measurements of Vandaele et al., 1998, and HCHO cross sections from Meller and Moortgat (2000). The PSI reference solar spectrum is constructed from a high resolution extraterrestrial spectrum from 270 nm to 1000 nm merged from different sources (Bernhard et al. (2004). Solar spectrum sources are from: Kurucz (2005) normalized to Thuillier et al. (2004), SUSIM/Atlas-3 spectrum (VanHoosier et al., 1996), and the spectrum from Gueymard (2004). One of the advantages of using direct-sun observations is the accurate conversion to vertical column based on a geometric calculation of the slant path air mass factor AMF for a known solar zenith angle SZA is with a slight correction to the function Secant(SZA) (Herman et al., 2009 eqn. 3). A complete description of the retrieval algorithms and PSI operations are given in the PSI software manual (Cede, 2017). Accuracy in the DOAS-type retrieval is obtained using careful measurements of the spectrometer's slit function, wavelength calibration, knowledge of atmospheric absorption cross sections, and the solar spectrum at the top of the atmosphere. Accuracy for C(NO<sub>2</sub>) has been estimated to be ±0.05 DU. A recent addition of anti-reflection coatings to the PSI optics has improved accuracy and precision by reducing the residuals associated with spectral fitting using trace gas absorption cross sections. The reduced residuals are necessary for the retrieval of formaldehyde and bromine oxide that absorb in spectral regions dominated by ozone and NO<sub>2</sub>. Other DOAS-type measurements have been made in Korea based on observations of sky radiance ratios (e.g., Multi Axis MAX-DOAS: Kanaya, et al., 2014) and direct-sun DOAS using a PSI in Seoul, Korea (Park et al., 2018)."

Since it is mentioned later on in Section 2 for the measurements in Anmyeondo, please discuss briefly the contribution of the stratosphere to the presented total vertical columns.

How large is the contribution and does it change over the day? Can stratosphere and troposphere be separated?

The measurement from the PSI is for total column (stratosphere + troposphere). For NO<sub>2</sub>, the stratospheric contribution is approximately 0.1 DU and it does change during the day by about 0.05 DU. The direct sun measurement does not permit separation of troposphere and stratosphere

A sentence was added, "Of these sites, Anmyeondo frequently (40%) retrieves values of C(NO2) that are close to the typical stratospheric values of 0.1±0.05 DU. Other sites occasionally have clean days with similar low values."

Please mention briefly what other work on ground-based (DOAS type) Korean/Asian air pollution measurements has been published in other studies in the past to put the aim of the campaign/study into context.

There are other DOAS measurements, but they are all MAX-DOAS, which are quite different than direct sun. I added a brief comment, "Other DOAS-type measurements have been made in Korea based on observations of sky radiance ratios (e.g., Multi Axis MAX-DOAS: Kanaya, et al., 2014) and direct-sun DOAS using a PSI in Seoul, Korea (Park et al., 2018)."

Fig. 2a, page 5: The agreement between the instruments is quite impressive. But what happened at 17:30-18:00 local time? Are these real differences or has the Pan27 instrument some missing data gaps and the connected data points convey a wrong impression?

These are differences caused by low signal from increasing cloud cover that affects the retrieval algorithm. There are small differences between instruments that introduce different amounts of noise in the signal for small signals.

Section 2, line 195f, page 8: See comment on stratospheric contribution above.

The most frequently occurring  $C(NO_2)$  value at Anmyeondo is 0.15 – 0.2 DU, which means that the measured  $NO_2$  amount are partly from the stratosphere (0.1±0.05 DU) with very little tropospheric or boundary layer  $NO_2$ . There are occasional  $C(NO_2)$  plumes that could be from industrial activity to the north, and, perhaps, from China. Transport of  $NO_2$  from China occurs episodically in significant amounts (Lee et al., 2014).

Section 3: Please explain in more detail why the observed NO2 daily patterns fit so well to automobile and power generation emissions.

The pattern measured by PSI in Korea during the spring KORUS-AQ campaign differed from other non-Korean locations in that there usually a weaker morning peak in Korea compared to the afternoon. The strong afternoon peak does not occur every day, but is often enough to be notable. The meteorological effects certainly play a role, but at this time the appropriate model studies are not available.

In many of the studies on the NO2 diurnal cycle in polluted urban regions two NO2 peaks in the morning and afternoon are observed corresponding to the morning and afternoon traffic rush hour. Do you have an explanation why the morning rush hour is hardly visible in the presented measurements and why the afternoon peak is so pronounced? Do you also observe a weekly cycle in your NO2 measurements, like it has been been observed in polluted regions and discussed for example in Beirle et al. (GRL, 2003) or lalongo et al. (AMT, 2016)?

Yes, there is a weekly cycle in that Sundays usually have less pollution than Wednesdays.

Section 4: About the seasonal cycles: Please discuss briefly why the seasonal cycle of NO2 has its minimum in August/September and its maximum in winter/early spring. Is there more heating during winter times in Korea or is it just due to less OH radicals because of less light in winter?

Winter in Korea is complicated with quite a bit of cloud cover and precipitation. This certainly would affect the chemistry. Plus the cold winter weather certainly increases the amount of energy used, which produces more NO2. Since I did not do the model studies, I preferred to just leave the data without a "hand waving" explanation.

Section 4, line 291, page 13: The "strong effect on local air quality" is an improvement of local air quality, right?

The strong effect on local air quality mentioned in the paragraph concerns large amounts of total column NO2, most of which is near the surface. This probably makes the air quality worse.

Section6, line531f, page27: What is the reason for this seasonal increase during May and June?

Unfortunately, there are no long term measurements of C(HCHO), so there is no way of determining if the increase is from sources or VOC chemistry. The PSI was not capable of measuring HCHO prior to late 2016.

### **Technical corrections:**

Line 43, page 2: please add "local time" or LT

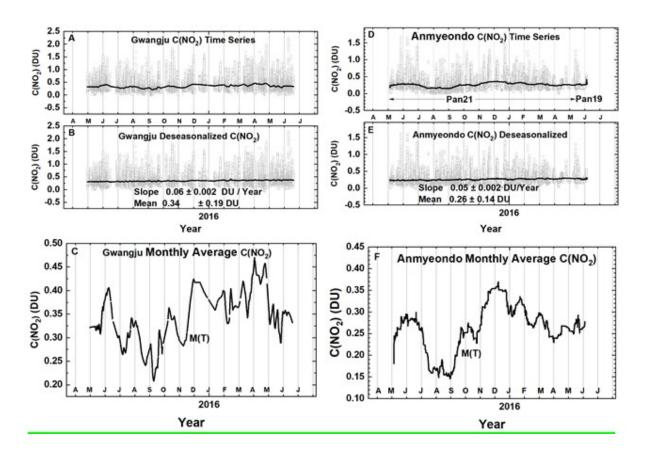
Added: "OMI overpass local times (LT =  $13.5 \pm 0.5$  hours)."

Line 48, page 2: please enclose "FOV" in brackets OK

Tab. 1: The degree symbol is missing for latitude and longitude values **OK** 

Line 229, page 10: Please round off the values for H2O and CO2. Six significant(?) digits are unnecessary here, since this paragraph is only about getting a general impression on the order of magnitude of the emissions from automobiles. **OK** "containing H2O (144 ppm) and  $CO_2$  (122 ppm)".

Fig. 6: Between Panel A and Panel B the x axis tick labels A, M, J and J (April, May, June, July) are missing.



Line 298, page 13: please add "local time" or LT Fig. 9a: Seoul (left panel): Why does the 3-month average (solid lines) show values where around 6 month of data are missing? Or is it just a linear interpolation between the values before and after the gap?

Missing data are represented by linear interpolation in the plots, but not any analysis. I have added a statement in the caption. "Fig. 9a Comparisons between the daily values of C(NO<sub>2</sub>) for OMI (black) and PSI (red) at Seoul and Busan for a 5-year period. Solid lines show the average seasonal variation (Lowess(0.1)), see also Fig. 9b. Linear interpolation is used where there are missing data points."

Line 429, page 19 and Fig. 14: The numbers in "Integ(0.026, 7.2)" are given in kilometers?

Yes. Added: "Integ(0.026, 7.2 km)"

Tab. 2.: "PSI HCHO" is missing the "DU" (like in "DC8 HCHO DU")

Table 2 is now

Table 2 Taehwa Mtn DC8 compared to PSI measurements (see 10 Jun in Fig. 18)

Date	LT	DC8 HCHO DU	PSI HCHO (DU)	Percent
11 May	08:25:19	0.4	0.6	67
18 May	08:34:26	0.4	0.5	80
30 May	12:05:00	0.5	0.9	56
10 Jun	08:22:45	1	1.16	86
10 Jun	12:22:53	1	1.5	67
10 Jun	15:46:03	1	1.3	77

Line 545, page 29: "... very high amounts of urban pollution from NO2 and HCHO \*, and more moderate, but still high values, away from the urban centers." \*close to the urban centers

**Changed to**," but still high values in Mt Taewha and Yeogju, which are some distance from the major urban centers,. An exceptional location was Amnyeondo"

1 2	NO <sub>2</sub> and HCHO measurements in Korea from 2012 to 2016 from Pandora Spectrometer Instruments compared with OMI retrievals and with aircraft measurements during the KORUS-AQ campaign
3 4	Jay Herman <sup>1</sup> , Elena Spinei <sup>2</sup> , Alan Fried <sup>3</sup> , Jhoon Kim <sup>4</sup> , Jae Kim <sup>5</sup> , Woogyung Kim <sup>3</sup> , Alexander Cede <sup>6</sup> , Nader Abuhassan <sup>1</sup> , Michal Segal-Rozenhaimer <sup>7,8</sup>
5	
6	
7	
8	
9	
10	
11	
12	
13	
14	
15	
16	
17	
18	Correspondence email: jay.r.herman@nasa.gov
19	<sup>1</sup> University of Maryland Baltimore County JCET
20	<sup>2</sup> Virginia Polytechnic Institute and State University, Blacksburg, VA 24061, USA
21	Institute of Arctic & Alpine Research, University of Colorado, Boulder, Colorado
22	<sup>4</sup> Dept. of Atmospheric Sciences, Yonsei University, Seoul Korea
23	<sup>5</sup> Department of Atmospheric Science, Pusan University, Busan, Korea
24	<sup>6</sup> Goddard Earth Sciences Technology & Research (GESTAR) Columbia, Columbia, MD 21046, USA
25	<sup>7</sup> Earth Science Division, NASA Ames, Mountain View, California
26	<sup>8</sup> Bay Area Environmental Research Institute, Petaluma, California
27	
28	

NO<sub>2</sub> and HCHO measurements in Korea from 2012 to 2016 from Pandora Spectrometer Instruments compared with OMI retrievals and with aircraft measurements during the KORUS-AQ campaign

31 32

29

30

### **Abstract**

33 34

35

36 37

38 39

40

41

42

43

44

45

46

47

48 49

50

51

52

53 54

55

56

57

58 59

Nine Pandora Spectrometer Instruments (PSI) were installed at 8 sites in South Korea as part of the KORUS-AQ (Korea U.S.-Air Quality) field study integrating information from ground, aircraft, and satellite measurements for validation of remote sensing air-quality studies. The PSI made direct-sun measurements of total vertical column NO<sub>2</sub>, C(NO<sub>2</sub>), with high precision (0.05 DU, where 1DU =  $2.69 \times 10^{16}$  molecules/cm<sup>2</sup>) and accuracy (0.1 DU) that were retrieved using spectral fitting techniques. Retrieval of Formaldehyde (HCHO) total column amounts were also obtained at five sites using the recently improved PSI optics. The HCHO retrievals have with high precision, but possibly lower accuracy than for NO2 because of uncertainty about the optimum spectral window for all ground-based and satellite instruments. PSI direct-sun retrieved values of C(NO<sub>2</sub>) and C(HCHO) are always significantly larger than OMI (AURA satellite Ozone Monitoring Instrument) retrieved C(NO<sub>2</sub>) and C(HCHO) for the OMI overpass local times (LT =  $13.5 \pm 0.5$  hours). In urban areas, PSI C(NO<sub>2</sub>) 30-day running averages are at least a factor of two larger than OMI averages. Similar differences are seen for C(HCHO) in Seoul and nearby surrounding areas. Late afternoon values of C(HCHO) measured by PSI are even larger, implying that OMI early afternoon measurements underestimate the effect of poor air quality on human health. The primary cause of the OMI underestimate is the large OMI field of view (FOV) that includes regions containing low values of pollutants. In relatively clean areas, PSI and OMI are more closely in agreement. C(HCHO) amounts were obtained for five sites, Yonsei University in Seoul, Olympic Park, Taehwa Mtn., Amnyeondo, and Yeoju. Of these the largest amounts of C(HCHO) were observed at Olympic Park and Taehwa Mountain, surrounded by significant amounts of vegetation. Comparisons of PSI C(HCHO) results were made with the Compact Atmospheric Multispecies Spectrometer CAMS during overflights on the DC-8 aircraft for Taehwa Mtn and Olympic Park. In all cases, PSI measured substantially more C(HCHO) than obtained from integrating the CAMS altitude profiles. PSI C(HCHO) at Yonsei University in Seoul frequently reached 0.6 DU and occasionally exceeded 1.5DU. The semi-rural site, Mt. Taehwa, frequently reached 0.9 DU and occasionally exceeded 1.5DU. Even at the cleanest site, Amnyeondo, HCHO occasionally exceeded 1 DU.

61

62

60

Keywords: Pandora, KORUS-AQ, NO2, HCHO, Formaldehyde, Korea

63

#### 1 Introduction

The purpose of this paper is to present the retrieved amounts of nitrogen dioxide and formaldehyde, NO<sub>2</sub> and HCHO, obtained from Pandora Spectrometer instruments (PSI) direct-sun observations during the KORUS-AQ campaign (Korea US Air Quality: May – June 2016). Quoting from a NASA website: "Korea U.S.-Air Quality (KORUS-AQ) is a joint field study between NASA and the Republic of Korea to advance the ability to monitor air pollution from space. The campaign will assess air quality across urban, rural and coastal South Korea using observations from aircraft, ground sites, ships and satellites to test air quality models and remote sensing methods. Findings will help develop observing systems using models and data to improve air quality assessments for decision makers." A thorough description of the KORUS-AQ campaign and its motivations is given in a pre-campaign white paper, https://espo.nasa.gov/korus-ag/content/KORUS-AQ. White Paper.

Assessing air quality in South Korea is of interest because of the levels of pollution arising from high densities of population and intense industrial activity associated with the production of  $NO_2$ . Recent measurements of surface concentrations of  $NO_2$  and comparisons with satellite data demonstrate the need for high quality ground-based measurements to augment satellite observations (Kim et al., 2017; Jung et al., 2017). The driving reason behind the interest is the effect of elevated levels of  $NO_2$  in Korea on human health (Kim and Song, 2017 and references therein). Measurements of  $NO_2$  from aircraft have been used to obtain altitude profiles to compare with data obtained from fixed site

measurements and to obtain a national scale

estimate of pollutant exposure (Lee et al., 2015;

Kim and Song, 2017).

In addition to NO<sub>2</sub>, PSI measurements were used to assess the amount of Formaldehyde (HCHO) present in the air. This is important because of HCHO potential impact on health (Zhang et al., 2013, ) and because it plays a strong role in tropospheric reactions leading to the formation of boundary layer ozone. Sources of HCHO are from atmospheric reactions with volatile organic compounds (VOC) emitted from ground sources and industrial activities (Lee at al., 2009). A previous paper describes HCHO retrievals from a PSI located at Yonsei University in Seoul using a similar spectral fitting retrieval algorithm used in the current study (Park et al., 2018), but using a different wavelength fitting range, 335 – 358 nm instead of 332 – 359 nm used in this study. The choice of spectral fitting

window is discussed in Spinei et al. (2018).



**Fig. 1** KORUS-AQ sites for 9 Pandora instruments at 8 sites.

As part of the KORUS-AQ campaign, a network of nine PSI was installed in Korea at 8 locations (Fig. 1 and Table 1). Five of the sites were selected to be "down-wind" from Seoul, an extremely NO<sub>2</sub> polluted area. The intent of the network was to integrate direct-sun column density observations of NO<sub>2</sub> and HCHO into a multi-perspective framework of observations including ground-based, satellite, and airborne measurements of air quality. Viewing air quality through these multiple perspectives is important for connecting observations from future geostationary satellites to air quality networks such that conditions both at the surface and aloft can be better understood and represented across unmonitored areas. The data are especially important for computer models used for forecasts and decision making. Five of the KORUS-AQ PSI had recently improved optics that permitted retrieval of total vertical column formaldehyde (C(HCHO)). Part of the network was installed in April 2015, a year before the start of the campaign. Three PSI continue to operate in Korea, one each, in Busan and Seoul since 2012, and one in Gwangju operating since April 2015.

Measurements of daytime total columns in Dobson Units, where 1 DU =  $2.69 \times 10^{16}$  molecules/cm<sup>2</sup>, C(NO<sub>2</sub>), C(O<sub>3</sub>) and C(HCHO) are obtained every 80 seconds, which enables the PSI to show rapid short term (minutes to hours) variations in most locations with significant pollution (e.g.,  $C(NO_2) > 0.2$  DU). PSI measurements of the visible and UV wavelengths are obtained separately (40 seconds each). A visible wavelength blocking filter, U340, reduces stray light for UV measurements.

Table 1 KORUS-AQ Locations (South to North)

Locations	Alt(m)	Latitude	Longitude
Gwangju	33	35.2260 <sup>0</sup> N	126.8430°W
Busan	228	35.2353 <sup>0</sup> N	129.0825 <sup>o</sup> W
Anmyeondo	41	36.5380 <sup>0</sup> N	126.3300 <sup>o</sup> W
Taehwa Mtn	160	37.3123 <sup>0</sup> N	127.3106 <sup>0</sup> W
Yeoju-1 & 2	90	37.3385 <sup>0</sup> N	127.4895 <sup>0</sup> W
Songchon	49	37.4100 <sup>0</sup> N	127.5600°W
Olympic Park	26	37.5232 <sup>0</sup> N	127.1260 <sup>0</sup> W
Seoul	181	37.5644 <sup>0</sup> N	126.9340°W

Details on the Pandora spectrometer instrument can be found in Herman et al., (2009 and 2015) as well as a NASA Pandora website

https://avdc.gsfc.nasa.gov/pub/DSCOVR/Pandora/Web\_Pandora/index.html and the data used are available from https://avdc.gsfc.nasa.gov/pub/DSCOVR/Pandora/DATA/KORUS-AQ/

The PSI consists of a small Avantes low stray light spectrometer (280 - 525 nm with 0.6 nm spectral resolution with 4 times oversampling) connected to an optical head by a 400 micron single strand fiber optic cable. The spectrometer is temperature stabilized at  $20^{\circ}$ C ( $68^{\circ}$ F) inside of a weather resistant container. The optical head consists of a collimator and lens giving rise to a  $1.6^{\circ}$  FOV (field of view) FWHM (Full Width Half Maximum) with light passing through two filter wheels containing diffusers, a UV340 filter (blocks visible light), neutral density filters, and an opaque position (dark current measurement). When the diffuser is used, the FOV is increased to over  $2^{\circ}$ . The optical head is

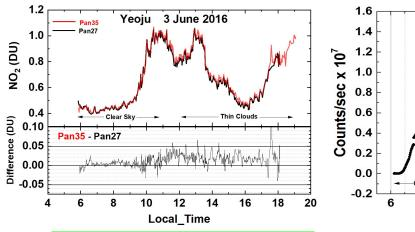
connected to a small suntracker capable of accurately following the sun's center using software running on a small computer-data logger contained in a weatherproof outer box along with the spectrometer in a second inner temperature controlled box. The PSI is capable of obtaining  $C(NO_2)$ , C(HCHO) and  $C(O_3)$  amounts sequentially over a period of 80 seconds including two dark current determinations. The integration time for  $NO_2$  in bright sun is about 4 milli-seconds that is repeated and averaged for 20 seconds (up to 4000 measurements) to obtain very high signal to noise ratios and very high precision (precision < 0.01 DU). Similar comments apply to C(O3), but not to C(HCHO), since formaldehyde absorption spectrum is mixed in with absorption from  $NO_2$  and  $O_3$ . This causes cross-correlation effects in the retrieval algorithm that make C(HCHO) retrievals sensitive to the selection of the wavelength range. The main source of noise in the measurement comes from the presence of clouds or haze in the FOV, which increases the exposure time and reduces the number of measurements in 20 seconds.

The retrieval algorithm is based a direct-sun spectral fitting method similar to the well-accepted DOAS (Differential Optical Absorption Spectroscopy, Platt, et al., 1979 and Platt, 1994). NO<sub>2</sub> absorption cross sections were obtained from the laboratory measurements of Vandaele et al., 1998, and HCHO cross sections from Meller and Moortgat (2000). The PSI reference solar spectrum is constructed from a high resolution extraterrestrial spectrum from 270 nm to 1000 nm merged from different sources (Bernhard et al. (2004). Solar spectrum sources are from: Kurucz (2005) normalized to Thuillier et al. (2004), SUSIM/Atlas-3 spectrum (VanHoosier et al., 1996), and the spectrum from Gueymard (2004). One of the advantages of using direct-sun observations is the accurate conversion to vertical column based on a geometric calculation of the slant path air mass factor AMF for a known solar zenith angle SZA is with a slight correction to the function Secant(SZA) (Herman et al., 2009 eqn. 3). A complete description of the retrieval algorithms and PSI operations are given in the PSI software manual (Cede, 2017). Accuracy in the DOAS-type retrieval is obtained using careful measurements of the spectrometer's slit function, wavelength calibration, knowledge of atmospheric absorption cross sections, and the solar spectrum at the top of the atmosphere. Accuracy for C(NO<sub>2</sub>) has been estimated to be ±0.05 DU. A recent addition of anti-reflection coatings to the PSI optics has improved accuracy and precision by reducing the residuals associated with spectral fitting using trace gas absorption cross sections. The reduced residuals are necessary for the retrieval of formaldehyde and bromine oxide that absorb in spectral regions dominated by ozone and NO2. Other DOAS-type measurements have been made in Korea based on observations of sky radiance ratios (e.g., Multi Axis MAX-DOAS: Kanaya, et al., 2014) and direct-sun DOAS using a PSI in Seoul, Korea (Park et al., 2018).

This paper discusses the distribution of C(NO<sub>2</sub>) and C(HCHO) over Korea at the sites where the PSI were located (Fig. 1). Section 2 shows the amounts of NO<sub>2</sub> observed by PSIs at the 8 KORUS-AQ sites. Section 3 discusses the diurnal variation of NO<sub>2</sub>. Section 4 looks at longer term changes in NO<sub>2</sub> obtained from PSIs that were deployed before the beginning of the KORUS-AQ campaign. Section 5 evaluates the disagreement with Ozone Monitoring Instrument (OMI) satellite C(NO<sub>2</sub>) retrievals (Kramer et al., 2008). Section 6 compared PSI C(NO<sub>2</sub>) retrievals with the aircraft overpass retrievals from the 4STAR instrument (Segal-Rozenhaimer et al., 2014). Section 6 discusses retrievals of C(HCHO) amounts for five PSI sites, the diurnal variation of C(HCHO), and comparisons with the Compact Atmospheric Multispecies Spectrometer CAMS (Richter et al., 2015) from DC-8 aircraft overflights of 5 PSI sites.

# 2 NO<sub>2</sub> during the KORUS-AQ Campaign (May – June 2016)

An example of NO<sub>2</sub> retrieval from two independently calibrated Pandoras that were initially located at the same site (Yeoju, Korea, 37.3385°N, 127.4895°W) are compared in Fig. 2a showing that the difference in C(NO<sub>2</sub>) amount is less than 0.05 DU even in the presence of thin afternoon clouds (Fig. 2b) that decrease the measured solar irradiance by more than a factor of 2. Though Yeoju is a relatively clean site in Korea (located to the southeast of Seoul Lat=37.5644°N, Long=126.934°W), C(NO<sub>2</sub>) amounts frequently reach moderately high values (e.g., 1 DU on 3 June 2016), and occasionally even higher (2-3 DU). However, Yeoju has much less C(NO<sub>2</sub>) compared to Seoul, less than 30 km distant, where PSI measurements were found to reach over 3 DU (Fig. 3) during the campaign period from mid-April to early June, 2016. Typical C(NO<sub>2</sub>) amounts are 0.3 to 0.5 DU in polluted regions.



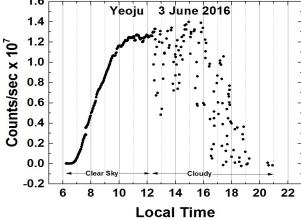


Fig. 2a  $C(NO_2)$  amounts from Pandora 27 and 35 in Yeoju, Korea during 3 June 2016 and their difference |Pan35 – Pan27| < 0.05 DU.

Fig. 2b Pandora 35 estimate of cloud or aerosol reduced measured counts/second at approximately 500 nm.

In a manner similar to Fig. 2a, C(NO<sub>2</sub>) amounts can show large variability from day-to-day and intraday, as well as between different sites. The largest amounts of C(NO<sub>2</sub>) are in the north (Seoul and Olympic Park) associated with the largest population and industry concentrations, while the southern cities of Busan and Gwangju have smaller amounts of C(NO<sub>2</sub>). The smallest C(NO<sub>2</sub>) amounts are at Anmyeondo (an island on west coast of Korea 42 km south of Seoul, usually not downwind of Seoul), and Songchon to the east of Seoul.

Figure 2b shows the effect of thin clouds in terms of reduced measured count rates for a single spectrometer pixel near 500 nm showing a near noon count rate of  $1.26 \times 10^7$  counts/second followed by a reduced count rate as clouds move in front of the sun. The cloud plus aerosol cover estimate is from the same date 3 June 2016 as the  $C(NO_2)$  amounts shown in Fig.2a. The effect of thin clouds for  $C(NO_2)$  retrieval (Fig. 2a) is increased noise (reduced precision) with a very small impact on accuracy. There are two effects on PSI observations to consider in association with thin clouds. First, is multiple

scattering within the cloud affecting the optical path and effective air mass factor AMF. This has a very small effect on AMF, since most of the  $NO_2$  is near the surface well below the clouds. Second, is the reduction in the number of measurements during a fixed 20 second measuring period causing a decrease in the signal to noise ratio. The weather during the campaign was occasionally very cloudy, which caused some missing  $NO_2$  and  $O_3$  data. However, most of the cloudy days were light to moderate cloud cover, which permitted  $C(NO_2)$  amounts to be determined, but with lower precision compared to clear-sky direct sun measurements (e.g., Fig.s 2a and b). When the cloud cover becomes sufficiently thick, precision is reduced (increased point-to-point scatter) and the spectral fitting error increases. A small percentage of data points with high retrieval error,  $C(NO_2 \text{ Error}) > 0.1 \text{ DU}$ , have been removed from the data set.

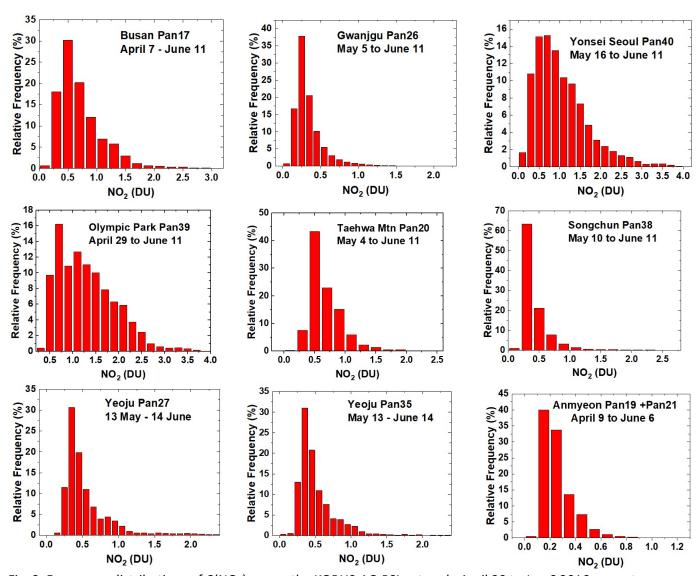


Fig. 3. Frequency distributions of  $C(NO_2)$  across the KORUS-AQ PSI network: April 20 to Jun 6 2016, except as labelled. The axes vary for different sites.

Figures 3 and 4 summarize all of the Pandora C(NO<sub>2</sub>) data obtained during the KORUS-AQ campaign. Figure 3 presents histograms in percent frequency of occurrence for all nine sites. All of the sites located within or downwind of major cities have production of NOx mainly from transportation and power generation as its major sources. The ratio of transportation NOx production compared to all other sources is estimated as up to a factor of three (Kim et al., 2013). Of these sites, Anmyeondo frequently (40%) retrieves values of C(NO2) that are close to the typical stratospheric values of 0.1±0.05 DU. Other sites occasionally have clean days with similar low values.

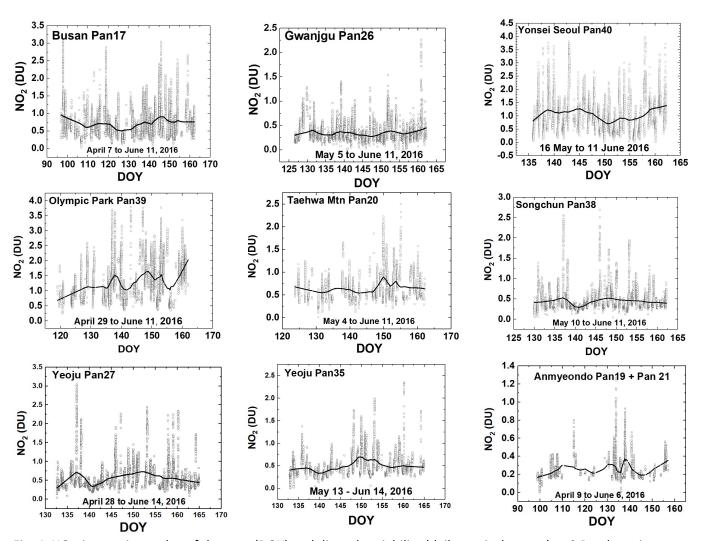


Fig. 4  $NO_2$  time series vs day of the year (DOY) and diurnal variability (daily vertical extent) at 9 Pandora sites. Notice the very high  $NO_2$  amounts in Seoul and nearby Olympic Park. The black curves are aproximately weekly least squares running averages. The daily vertical extent corresponds to diurnal variation (Fig. 2). Note: the vertical scales are different for each site to show the daily variability relative to the running average.

The Seoul site frequently has amounts of  $C(NO_2)$  greater than 2 DU. The same is true of Olympic Park, located in the eastern part of the Seoul metropolitan area. For locations increasingly distant from Seoul, the amount of  $C(NO_2)$  decreases in response to smaller local emissions, since the short chemical lifetime of  $NO_2$  normally precludes long distance transport. Compared to Seoul, the two smaller southern cities, Gwangju and Busan, have relatively low levels of  $C(NO_2)$  on most days, with the most typical values ranging from 0.3 to 0.5 DU, although high values exceeding 2 DU can occur on rare occasion.

Figure 4 shows the same data as Fig. 3, but in the form of a time series covering the KORUS-AQ period. The daily variation (at least one point every two minutes) is shown in the vertical extent corresponding to each day's data. Figures 3 and 4 show that sites near Seoul metropolitan (Olympic Park) area have larger amounts of pollution compared to those further away (Taehwa, Songchon, and

Yeoju). Even though average  $C(NO_2)$  amounts are much lower at Songchon and Yeoju, there are times when the pollution levels are quite high  $(C(NO_2) > 2 DU)$ , Figs. 4 and 5). There are days when the amount of  $C(NO_2)$  gets close to 4 DU in Seoul, 3 DU in Olympic Park and Busan, and 4 DU for one day in Yeoju (April 27). The southern cities, Busan and Gwangju are much less polluted on average, which results in a much smaller effect on adjacent regions. Busan is located on the southeastern coastline, so that some of its  $NO_2$  pollution dissipates over the ocean, except for occasional days when very high amounts (3 DU) occur. Anmyeondo is quite clean, since it is located on the western coast well south of Seoul. The most frequently occurring  $C(NO_2)$  value at Anmyeondo is 0.15 - 0.2 DU, which means that the measured  $NO_2$  amount are partly from the stratosphere  $(0.1\pm0.05 DU)$  with very little tropospheric or boundary layer  $NO_2$ . There are occasional  $C(NO_2)$  plumes that could be from industrial activity to the north, and, perhaps, from China. Transport of  $NO_2$  from China occurs episodically in significant amounts (Lee et al., 2014).

# 3 Diurnal Variation of C(NO<sub>2</sub>)

Grouping the diurnal variation together from multiple days (Fig. 5) reveals a pattern to  $NO_2$  emissions and accumulation related to the main  $NO_2$  emission sources (automobiles and power generation) for the 3 largest cities in Korea: Seoul (Pan40), Busan (Pan17), and Gwangju (Pan26). For Seoul, the amounts of  $C(NO_2)$  during the morning (1 DU at 10:00) are much less than later in the afternoon (over 2 -3 DU at 16:00) on almost every day with values occasionally reaching as high as 6 DU. Even the relatively low morning values of  $C(NO_2)$  represent a significant amount of pollution. The 6 DU  $C(NO_2)$  amount in Seoul is unusual, but coincides with the peak values frequently occurring in the late afternoon.  $C(NO_2)$  behavior at nearby Olympic Park to the east of Seoul is very similar to Yonsei University in the heart of Seoul, even though Olympic Park's traffic density is lower than Seoul. Olympic Park is close enough to the metropolitan Seoul area for the transport of  $NO_2$  combined with local production from traffic to produce a very similar diurnal pattern. The moderately large city of Busan also has high values of  $NO_2$ , occasionally reaching 3 DU in the afternoon. Busan has relatively low values of  $NO_2$  in the morning, having peaks in the mid-afternoon and declining in the late afternoon. Gwangju, located in the southwest, is a smaller city with less pollution (peak values = 1.6 DU) and does not have as distinct an afternoon maximum.

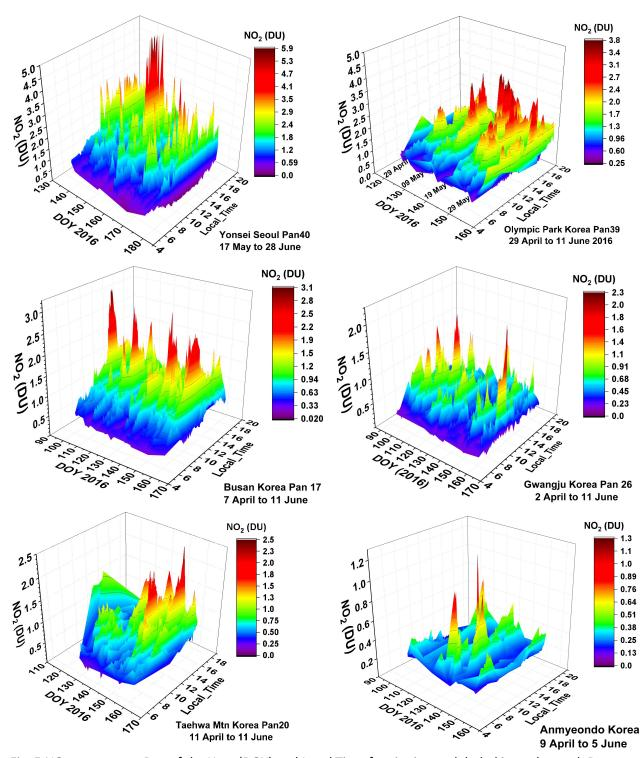


Fig. 5  $NO_2$  amounts vs Day of the Year (DOY) and Local Time for six sites as labeled in each panel. Day 120=April 29, Day 130=May 9, Day 140=May 19, Day 150=May 29, Day 160=June 8, Day 170 =June18.

The panels in Fig. 5 for Taehwa Mtn. and Anmyeondo show regions outside the Seoul metropolitan area that still show substantial amounts of NO<sub>2</sub>. Compared to Seoul, the Taehwa site is a semi-rural location with only a small amount of car traffic in the immediate area. However, there are major highways about 6 km from the site that are close enough to permit transport of NO<sub>2</sub> to the Taehwa Mountain site. All of the sites showed a tendency to have peak NO<sub>2</sub> occur in the late afternoon. Anmyeondo on the west central coast of Korea shows C(NO<sub>2</sub>) amounts that are quite low with occasional plumes arriving from the north or the west (China).

The basic daily pattern of C(NO2) in urban Korea arises from large amounts of automobile traffic and power plants emitting  $NO_X$  (for modern automobiles, roughly 99 % NO and 1 %  $NO_2$ ). An FTIR analysis of automobile exhaust shows that NO is emitted at 127 ppm,  $NO_2$  at 1.6 ppm, HCHO at 39 ppm, and  $CH_3OH$  at 139 ppm as part of the main emissions containing H2O (144 ppm) and  $CO_2$  (122 ppm). (https://tools.thermofisher.com/content/sfs/brochures/D10248~.pdf); see also Walters et al., 2015).

NO quickly converts into  $NO_2$  in the presence of ozone and volatile organic compounds VOCs in the atmosphere and can convert back to NO by solar photolysis. KORUS-AQ results frequently show increasing  $NO_2$  during the day with peaks in the afternoon. For these days the measurements imply that the amount of locally produced  $NO_X$  and conversion into  $NO_2$  dominates the losses of  $NO_2$  by photolysis and transport out of the region. Other days occasionally show a different behavior, with  $NO_2$  peaks in the morning and a decline thereafter suggesting transport out of the region.

# 4 Longer-Term Changes in C(NO<sub>2</sub>)

Some of the sites used for the KORUS-AQ campaign (Gwangju and Amnyeondo) had PSIs set up in April 2015, about one year before the start of the campaign. Two other sites (Seoul and Busan) have PSI  $C(NO_2)$  data starting in 2012. The extended data sets for Seoul and Busan provide the opportunity to estimate 5-year changes in  $C(NO_2)$  amount and seasonal dependence.

In Fig. 6, the daily variation over one year at Gwangju and Anmyeondo are evaluated to estimate one year secular trends. The vertical extent in the time series is not noise or uncertainty, but rather the 80 second per data point variability throughout each day (e.g., see Fig. 2). Before calculating linear least squares slopes, the unadjusted time series (grey data points in Panels A and D) were deseasonalized (grey data points in Panels B and E) by subtracting a function with zero slope derived from a 30 day running average (dark line in panels A and D or the identical curves in C and F). The running average curves in panels A and D are shown with expanded scale in panels C and F to clearly show the seasonal variation. The "zero slope functions" ZM(t) are obtained by subtracting a linear least squares fit L(t) to monthly running average curves M(t) in panels C and F to form zero slope functions ZM(t) = M(t) - L(t). The results ZM(t) are functions that look similar to the M(t) plots in panels C and F, but with zero slopes. The resulting ZM(t) are then subtracted from the respective original time series (grey circles) in panels A and D. The results are the grey circles in Panels B and E. Similar monthly running means are shown in Panels B and E that have almost no monthly variations (see appendix Fig. A1).

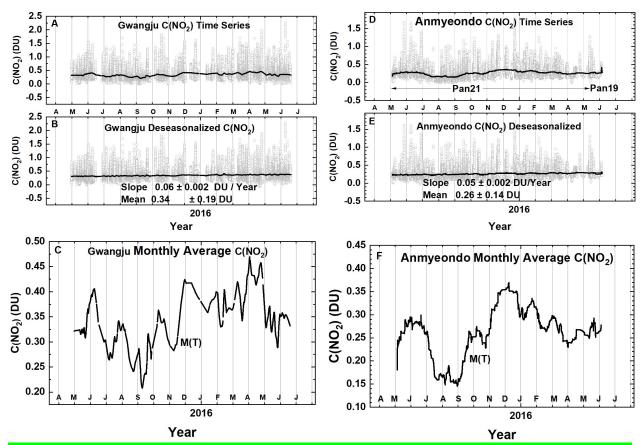


Fig. 6 Approximately 1 year of daily column C(NO<sub>2</sub>) amount data (Panels A and D) and the monthly running average amount (dark plot in Pandels A and D). The data are from GIST at Gwangju and Amnyeondo. Panels A and D are the original time series with one data point every 80 seconds, panels B and E are the deseasonalized time series. Panels C and F are an expanded scale of the monthly running averages M(t) of C(NO<sub>2</sub>) that are identical to the solid lines in panels A and D. The vertical extent (panels A, B, D, and E) on a given day is the range of diurnal variation from early morning to late afternoon.

The linear trends in Figs. 6B and 6E suggest that there was an increase in pollution levels in Gwangju and Anmeondo over the period of observation. The southern city of Gwangju (Pan 26) has higher average  $C(NO_2)$  amounts,  $0.34\pm0.19$  DU, compared to the relatively clean coastal site Amnyeondo,  $0.26\pm0.14$  DU. Gwangju seasonal cycle has a minimum in  $C(NO_2)$  amount in September-October and a very broad maximum from December to May. The Gwangju PSI is located away from major city traffic on a university campus (Gwangju Institute of Science and Technology, GIST) so that the average amount of  $NO_2$  (about 0.34 DU) is moderate with some days reaching 1.5 DU. The slopes are statistically significant at the 2-standard deviation level (p < 0.05) and imply that  $C(NO_2)$  was increasing at a substantial rate However, the period of observation was too short to estimate multi-year long-term trends. Additional long-term monitoring of these sites would be desirable for air quality purposes.

The PSI on Anmyeondo was located away from a commercial area with moderate traffic and very near the shore of the Yellow Sea at a regional Global Atmosphere Watch (GAW) station. For Amnyeondo there is a clear seasonal cycle similar to that in Gwangju with a minimum in September-

October and a broad maximum during the winter-spring months. Amnyeondo had an average amount of 0.25 DU, which is lower than observed at Gwanjgu.

317

318

319

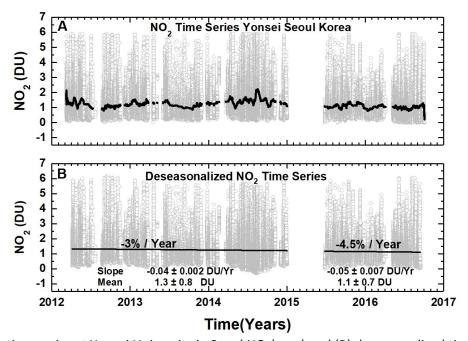


Fig. 7 (A)  $NO_2$  time series at Yonsei University in Seoul  $NO_2$ (grey) and (B) deseasonalized time series. Combined slope =  $-0.05 \pm 0.001$  DU/Year and Mean =  $1.2 \pm 0.8$  DU or the decrease is  $-4 \pm 0.08$  % / Year. Seoul has no clear seasonal cycle.

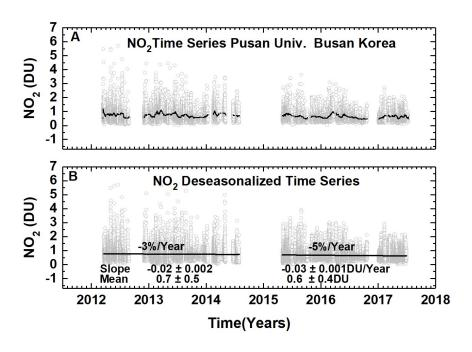


Fig. 8 (A) Pusan University in Busan NO<sub>2</sub> daily time series (grey) and (B) deseasonalized time series with linear trends.

Figures 7 and 8 each contain an approximately 5-year daily time series (grey) for Seoul (Yonsei University) and Busan (Pusan University) and a linear fit to a deseasonalized version of the time series. Since the observations at both sites had an extended period of missing data, the slopes were estimated separately for each segment and for the combined time series. Both Seoul and Busan show a steady reduction in  $NO_2$  air pollution with an average reduction of about -4 % per year. A recent paper by Duncan et al., (2016) estimated a decrease in  $C(NO_2)$  for Seoul in about a 10 x 10 km box of about 1.6  $\pm$  1.4 % per year over the 2004 to 2013 period based on a 2014 average  $C(NO_2)$  amount of 0.6 DU, or about half of the average value 1.3  $\pm$  0.8 DU observed by the PSI. The larger reduction in  $C(NO_2)$  measured by the PSI is caused by a reduction in higher than average afternoon  $C(NO_2)$  amounts that are rarely observed by OMI overpass at 13:30 local time. OMI is a polar orbiting push broom hyperspectral instrument (300 – 500 nm with resolution of 0.45 nm in the UV and 1 nm in the visible and a spatial resolution of 13 x 24 km²) onboard the AURA satellite. The high observed late afternoon values are not restricted to Seoul, but occur for all of the urban areas where the PSI has been deployed. The high late afternoon values do not regularly occur in remote rural areas such as Amnyeondo.

Seoul and Busan  $C(NO_2)$  measurements are remarkable for the large peak amounts that are seen on most days compared to the 1.5 to 2 DU peak values for Gwangju and Amnyeondo. For Yonsei, the peak values range above 5 to 6 DU in the years 2012 to 2015, but decrease somewhat in 2015 to 2016. In 2015 - 2016, the decrease appears to be large, but is only 0.2 DU relative to a mean of about 1.2 DU. A smaller decrease appears for Busan (Fig. 8) relative to a mean of about 0.6 DU. All of the PSI measurements show very high values of  $NO_2$  during almost every day when measurements were possible. Since the  $NO_2$  concentrations represented by these large column amounts are probably in the boundary layer near the sources of  $NO_2$ , there is a strong effect on local air quality.

# 5 Comparison with OMI Satellite Overpass Data

Seoul and Busan have 5-year PSI data records (Figs. 9a and 9b), and Gwangju has a 1-year data record (Figs. 6 and 10) spanning the KORUS-AQ campaign. The PSI  $C(NO_2)$  can be matched in time ( $\pm$  8 minutes) with the overpass time from OMI (Ozone Monitoring Instrument) onboard the AURA satellite (mid-day overpass times  $13:30 \pm 90$  minutes). Figure 9a shows the  $C(NO_2)$  daily variation at the OMI overpass time with far more high values of  $C(NO_2)$  from the PSI than observed by OMI. The solid lines represent the seasonal dependence, which are shown separately in Fig. 9b along with the  $C(NO_2)$  differences, PSI - OMI. The result is that the average PSI values are double those observed by OMI's large FOV. (OMI Version 03: https://avdc.gsfc.nasa.gov/index.php?site=666843934&id=13)

The seasonal dependence (Fig. 9b) of C(NO<sub>2</sub>) from OMI for both Seoul and Busan is fairly regular, with maxima in January of each year and minima in July-August. The seasonal behavior of C(NO<sub>2</sub>) obtained from the PSI for Seoul varies with high values extending from January into the summer months and with minima varying from August in 2012, September-October in 2013, missing in 2014, July in 2015, and June in 2016. For Busan, the maxima occur in the Spring for 2013 and 2014, October for 2015, and in the Spring for 2016. The minima are also variable. The difference between OMI and PSI retrievals depends on local conditions for PSI and on an area average for OMI.

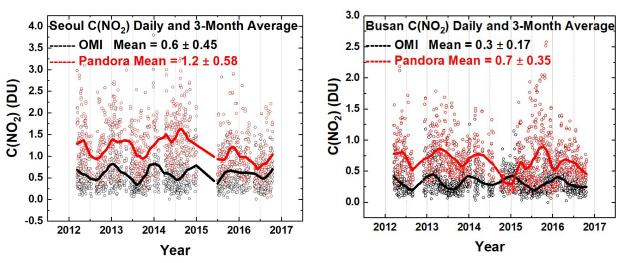


Fig. 9a Comparisons between the daily values of  $C(NO_2)$  for OMI (black) and PSI (red) at Seoul and Busan for a 5-year period. Solid lines show the average seasonal variation (Lowess(0.1)), see also Fig. 9b. Linear interpolation is used where there are missing data points.

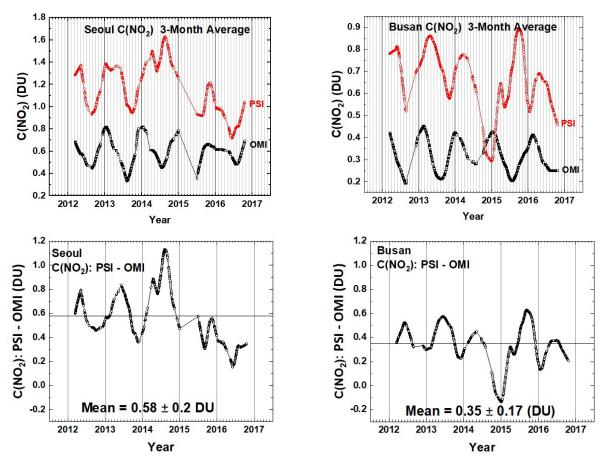


Fig. 9b Comparisons between the seasonal averages for  $C(NO_2)$  from OMI (black) and PSI (red) at Seoul and Busan for a 5-year period. The lower panels show the seasonal difference between the PSI and OMI. The individual data points are shown derived from a Lowess(0.1) smoothing, approximately a 3-month running averages of the daily data. Interpolation used where there are missing data points.

Figure 9b shows that the PSI has a mean difference compared to OMI in Busan of 0.35 DU and peak values (up to 2.5 DU at 13:30 and 4 DU in the late afternoon). The differences are important when considering pollution effects on human health (Krafta et al., 2005; Latza et al., 2009). Even larger differences are observed in Seoul, where the mean difference is 0.58 DU between Pandora and OMI at the satellite overpass time. The results from PSI suggest that local ground-based monitoring of pollution is important for estimating their impact on human health, particularly since amounts of C(NO<sub>2</sub>) occurring later in the afternoon exceed the amounts at the time of the satellite overpass.

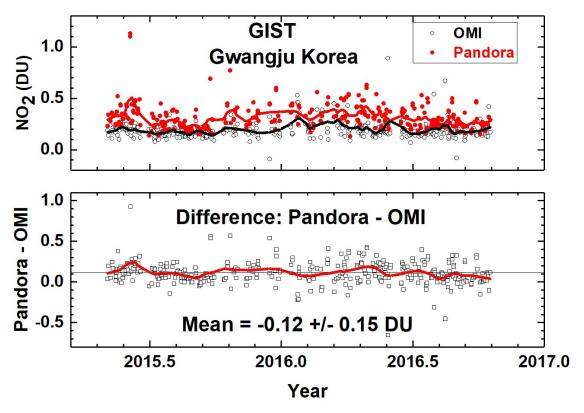


Fig. 10 C(NO<sub>2</sub>) time series from Pandora (red) and OMI (black) for GIST University in Gwangju Korea and their differences. The comparison is formed from time coincidences between Pandora and OMI.

A comparison with Lowess(0.1) fits (Locally Weighted least squares fit to 0.1 of the data points, (Cleveland, 1981)) to the matched Pandora vs OMI overpass data (about 3-month averages) shows that PSI C(NO<sub>2</sub>) is larger than OMI measured C(NO<sub>2</sub>) mostly because of its much smaller  $2^{\circ}$  field of view (a circle of 35 meters diameter at 1 km altitude) compared to OMI's FOV of 13 x 24 km<sup>2</sup> at nadir, which may encompass areas outside of the city or the adjacent ocean areas. For example, the center of Seoul is about 48 km from the Yellow Sea, while the OMI overpass file lists FOV center distances of over 60 km from Seoul. Another possible reason for the differences is that OMI C(NO<sub>2</sub>) retrievals use NO<sub>2</sub> vertical profile shape factors from the low resolution (~110 × 110 km) Global Model Initiative (GMI) model simulation to calculate air mass factors that are used to determine observed tropospheric NO<sub>2</sub> vertical columns, while much finer resolution profiles are needed to more accurately represent highly polluted

urban areas such as Seoul. Increases in OMI retrieved tropospheric column  $NO_2$  up to 160 % are found when using model derived 1.33 x 1.33 km<sup>2</sup> profile shape factors (Goldberg et al., 2017). The effect of moderate amounts of cloud or aerosol have little effect on the PSI direct -sun spectral fitting retrieval of  $C(NO_2)$  as shown in Fig. 2. OMI and MAXDOAS retrievals are sensitive to the presence of aerosols and clouds (Kanaya et al., 2014), which may contribute to the underestimate of  $C(NO_2)$  by OMI even after corrections are made for retrieved aerosol and cloud amounts (Chimot, et al. 2016).

The implications for assessing clean air indices suggest that OMI underestimates the human health effect from trace gases such as NO<sub>2</sub>, especially in highly populated urban areas. Figure 5 gives a much clearer picture of the degree of pollution than is possible with just the 13:30 OMI comparison measurements, since the late afternoon is the time of maximum pollution.

The city of Gwangju is much smaller than Busan, with less industrial activity, especially automobiles. PSI observations at GIST show much closer agreement with OMI (Fig. 10), especially since GIST is located within the city boundaries, but in an area with much less concentrated industrial activity compared to the center of Gwangju. The large OMI FOV over a relatively clean area reduce the OMI difference in measured  $NO_2$  amount compared to the PSI  $C(NO_2)$  amounts. OMI still measures less than the PSI  $(0.12 \pm 0.15 \ DU)$ , but the mean difference is not statistically significant. However, OMI clearly misses the high values of  $C(NO_2)$  that are present in the PSI observations.

### 5.1 Comparison with 4STAR DC-8 Overpass Data

 $C(NO_2)$  results were obtained by the Spectrometer for Sun-tracking Sky-Scanning Atmospheric Research (4STAR) flown on-board the DC-8 during KORUS-AQ and compared with the PSI (Fig. 11). The 4STAR is an airborne sunphotometer, capable of measuring total  $C(NO_2)$ ,  $C(O_3)$ , water vapor and AOD columns in its direct-sun mode (Segal-Rozenhaimer et al., 2014; Shinozuka et al., 2013), which is similar to the mode used by the PSI network.

A detailed description of 4STAR is given in Dunagan et al., (2013). In brief, the instrument has two structurally rigid grating array spectrometers that are combined to yield continuous spectra between 300-1700 nm. The instrument sampling rate is 1 Hz, and the nominal integration time used for C(NO<sub>2</sub>) retrievals is 50 ms (with six spectra averaged per one sampling period). Dark counts are measured every 20 min using a shutter mechanism. The 4STAR light collection system has fiber optic bundle foreoptics that is connected to the spectrometers. A two-axis motion control system with analog feedback provides active tracking of the solar disk. The instrument full field of view (FOV) is ~1.25°. C(NO<sub>2</sub>)is retrieved following a method described in Segal-Rozenhaimer et al. (2014), but using the 460-490 nm spectral range. A series of 4STAR columnar NO<sub>2</sub> values above aircraft (for legs below 300 m) taken from DC8 "missed approach" maneuvers overflying Olympic Park PSI station, within a radius of 5 km, are shown in Fig. 11. There is a relatively good correlation (R<sup>2</sup>=0.7), with a slight positive bias of 4STAR compared with the PSI values. This might result from higher noise effects (i.e. small amount of spectra averages) for 4STAR during the fast change of altitude when the aircraft performs its "missed

approach" overpasses over the PSI stations. Relaxing the altitude constraint to include legs below 500 m showed good agreement with the PSI station at Taewha Mountain, but with an overall lower correlation coefficient (R<sup>2</sup>=0.54), which is expected due to averaging of larger vertical range. As with PSI, 4STAR shows better agreement with OMI C(NO<sub>2</sub>) for low values of C(NO<sub>2</sub>), but considerable differences over polluted areas (Segal-Rozenhaimer et al., *in prep.*), when 4STAR C(NO<sub>2</sub>) values are averaged within each of the OMI pixels corresponding to the flight path for each of the days.

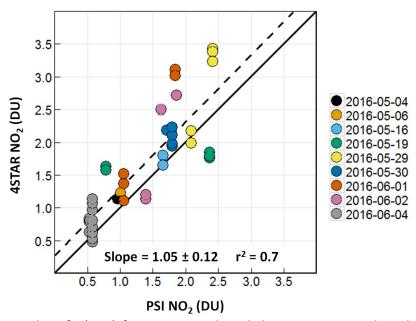


Fig. 11 A correlation plot of  $C(NO_2)$  from 4STAR onboard the DC-8 compared to the  $C(NO_2)$  amount measured by the PSI at Olympic Park on nine different days. The solid black line is the 1:1 line drawn for reference. The dashed line represents the data linear fit, with a slope of 1.05, and a correlation coefficient  $r^2 = 0.7$ , as shown on the plot.

### 6 Formaldehyde from Five Korus-AQ Sites

PSI makes two sets of direct-sun measurements every 80 seconds. One set is for measurements in the visible range (380-525 nm used for  $NO_2$ ) and the other is for the UV range (290-380 nm with a filter, U340, which blocks visible light). Formaldehyde is derived from the same set of spectral measurements used for ozone (i.e., with a U340 blocking filter), but using the spectral range 332-359 nm. Sources of error in the C(HCHO) retrieval arise from the selection of the fitting window and the amount of C(HCHO) remaining in the reference spectrum after application of the modified Langley estimation (MLE) method of calibration (Herman et al., 2009, Spinei et al., 2018). The MLE extrapolation to zero C(HCHO) could have an offset error of 0.1 to 0.2 DU. Selecting different fitting windows can also cause the C(HCHO) retrievals to differ. For example, a wider alternate fitting window, 324-360 nm, retrieves HCHO values that are about 8% higher because of different amounts of interference from overlapping absorption by  $O_3$ ,  $NO_2$ , and BrO at the spectral resolution of 0.5 to 0.6 nm currently in use.

Absolute offset errors do not affect the retrieval precision (relative column amounts), which is approximately 0.1 DU. A detailed analysis of the algorithms and uncertainties is discussed by Spinei et al., 2018.

The Olympic Park area has much more vegetation than central Seoul for the production of isoprene (<a href="http://www.olympicpark.co.kr">http://www.olympicpark.co.kr</a>), which is a significant source of the chemicals needed for formaldehyde production in the atmosphere (Luecken et al., 2012). Observations from PSI show that C(HCHO) starts out every day at low levels 0.6 DU at about 08:00 and increases to over 2 DU until 18:00 (Fig.s 12 and 13). Most HCHO arises from photochemical production, while a significant fraction is chemically derived from automotive emissions in densely populated urban areas (Friedfeld et al., 2002; Garcia et al., 2006; Lei et al., 2009; Liteplo et al., 2010). Regardless of the precursor source, HCHO forms in the atmosphere primarily by photochemistry, which causes HCHO to usually be a minimum early in the day, increase into the afternoon, and decline towards evening. The PSI C(HCHO) observations (Figs. 12 and 13) support this pattern of daily variation.

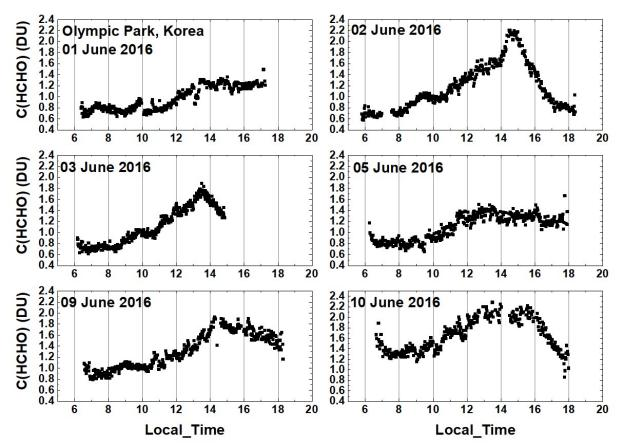


Fig. 12 C(HCHO) from PSI at Olympic Park for 6 days in June 2016. C(HCHO) on 2 June 2016 has a peak value of 2.3 DU at 14:30 hours.

A summary of the daily time dependence of C(HCHO) at Olympic Park during the entire KORUS-AQ campaign is shown in Fig. 13. As in Fig. 12, minimum values are observed in the

morning (06:00 – 08:00) before the chemical and direct sources of HCHO are significant. There is strong buildup during the day that reached a maximum between 15:00 to 16:00, and then diminished towards sunset. As with  $NO_2$ , the daily pattern of late afternoon peaking of HCHO amounts presents a problem for polar orbiting satellite observations (e.g., OMI observations at 13:30) assessing air quality.

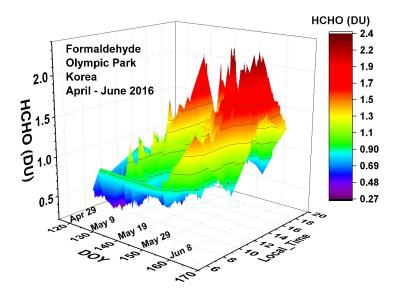


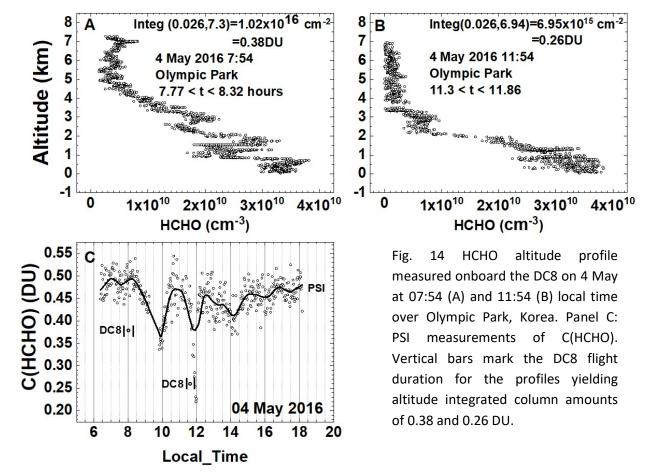
Fig. 13 Pandora measured formaldehyde amounts vs day of the year and local time for 29 April 2016 to 11 June 2016 in Olympic Park.

Figure 14 shows two altitude profiles acquired by the Compact Atmospheric Multispecies Spectrometer (CAMS) (Richter et al., 2015) onboard the DC-8 aircraft as it spiraled over the Olympic Park area on 4 May 2016 in the morning and at midday. Quoting from Richter et al., (2015), "CAMS is a multi-species spectrometer configured for the simultaneous detection of ethane (C2H6) and formaldehyde (CH2O). The spectrometer utilizes a tunable, fiber optically pumped difference frequency generation laser source in combination with a Herriott type multi-pass absorption cell with an effective path length of 89.6 m"

 The morning integrated amount on 4 May was  $1.02 \times 10^{16}$  molecules cm<sup>-2</sup> (0.38 DU) and the afternoon amount was  $6.95 \times 10^{15}$  molecules cm<sup>-2</sup> (0.26 DU), both substantially less than the PSI measured values of 0.48 DU and 0.42 DU, respectively. There were no surface measurements of HCHO mixing ratio on 4 May at Olympic Park. On 2 June at 11:40 there was a surface measurement 3.94 ppb. Including the surface measurement in the profile integral yields Integ(0.026, 7.2 km) = 0.55 DU, while PSI

measured 1.2 DU, which is consistent with the differences shown in Fig. 14. The notation in Fig 14 is  $Integ(z1,z2) = \int_{-z_0}^{z_0} HCHO(z)dz \text{ for the altitudes } z1 \text{ to } z2.$ 





The profiles used data for lower altitudes obtained from aircraft "missed approach" maneuvers at a nearby Seoul Airbase, 8.5 km from Olympic Park, (Fig. 15). When available, a single surface altitude point was added using ground-based volume mixing ratio measurements obtained from US Environmental Protection Agency measurements using quantum cascade laser instruments (Hottle et al., 2009, Spinei et al., 2018 and references therein). The DC-8 minimum altitude exactly over Olympic Park was typically around 0.4 km above the surface (black circles Fig. 15). Large vertical DC-8 HCHO gradients were observed as the DC8 descended to lower altitudes over Seoul Airbase. A comparison of 10-second DC-8 HCHO averages at the points of closest spatial approach to the Olympic Park (black circles) site on June 4, for example, to peak HCHO measurements during missed approaches at the nearby Seoul Airbase (20 – 40 meters above the ground) revealed ratios in the observed HCHO (black circles) ranging between75 % to

83 % of the maximum values near the surface. Since Olympic Park DC-8 overpasses miss significant near surface HCHO amounts, the profiles shown in Figs. 14 and 16 incorporate the HCHO amounts down to the surface at an altitude of 0.026 km asl derived from the "missed approach" at Seoul airbase. HCHO measurements above the maximum altitude over Olympic Park (see Fig. 14 and 16) were taken from the closest time over the Taewha Mtn. site, 28 km from Olympic Park. The assumption is that the horizontal gradients above 2.2 km (Fig. 15) can be neglected,

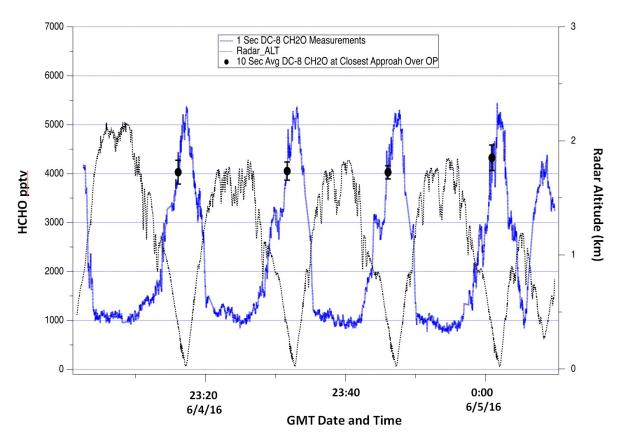
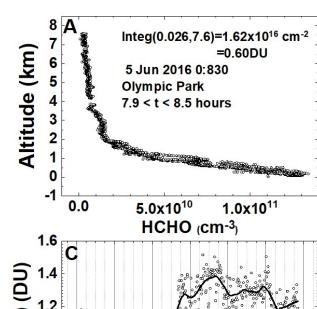
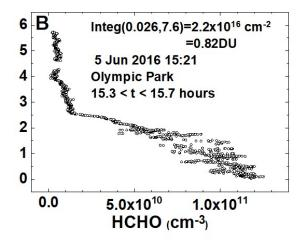


Fig. 15 DC-8 HCHO measurements over Olympic Park on June 4. The continuous blue profiles show the 1-second HCHO data while the black points with error bars show the 10-second average and standard deviation of this data at points of closest approach above the Olympic Park site.

After conversion from mixing ratio to molecules/cm<sup>3</sup> using the measured atmospheric density, the resulting profile data were integrated from the minimum (0.026 km asl, Table 1) to the maximum heights indicated in Fig. 14. The result is 0.38 DU at 07:54 and 0.26 DU at 11:54 compared to the measurements from the Pandora instrument 0.48 and 0.38 DU The derived vertical HCHO columns from the DC8 data in Fig. 14 A and B are 79 % of PSI measured C(HCHO)in the morning and 68 % of PCI C(HCHO) at midday (Fig 14 C).

A similar comparison is shown in Fig. 16 for 5 June 2016 where the amount of C(HCHO) is much larger than on 4 May. Integration of the measured profiles yields column densities of 0.60 and 0.82 DU at 08:30 and 15:21 hours. For this case, at both times the DC8 values are about 77 % and 63 % of the PSI measured column amounts, 0.78 and 1.3 DU. For both cases in Figs. 14 and 15 the 23 % to 37 % differences are outside of the expected error from PSI fitting window selection and from residual HCHO included in the MLE calibration method.





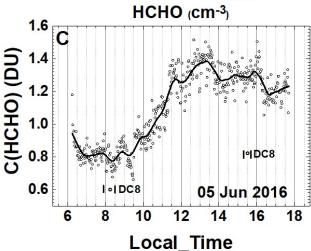


Fig. 16 HCHO altitude profile measured onboard the DC8 on 5 June at 8:30 (A) and 15:21 (B) local time over Olympic Park, Korea. Panel C: PSI measurements of total column HCHO. Vertical bars mark the DC8 flight duration for the profiles yielding column amounts of 0.60 and 0.82 DU.

Another Olympic Park case on 9 June 2016 shows DC8=0.79 vs PSI=1 DU at 08:06, DC8=0.74 vs PSI=1.3 DU at 12:12, and DC8=1.13 vs PSI=1.9DU, or the DC8 measurements are 79 % and 57 % less than the PSI total column HCHO. All of the remaining comparisons of DC8 profile results with PSI C(HCHO) show similar results. The reasons for the disagreement between C(HCHO) measured by direct sun observations (PSI) and the integrated column density from aircraft measurements of HCHO VMR are not known. Contributions to the differences include the selection of the PSI wavelength window (332 - 359 nm) and possible interference from overlapping  $NO_2$  and  $O_3$  absorption that are not properly included, and, more likely, the use of CAMS measured volume mixing ratios at the lowest altitudes from the nearby Seoul airbase, 8.5 km from Olympic Park, where spatial

variation may affect the calculation of C(HCHO). The use of Taehwa Mtn. data for higher altitudes over Olympic Park contributes 25 % for 3 of the above cases and 50 % for 4 May 2016 at 07:54 (Fig. 14A). This is probably not the reason for the disagreement between CAMS and PSI, since the percent underestimate for CAMS over Taewha is about the same magnitude (Table 2) as over Olympic Park.

PSI measurements show that Olympic Park produces more HCHO almost every day than observed at the Yonsei University in Seoul and Taehwa Mountain sites (Figs. 12, 17, 18). The hourly variations observed during the KORUS-AQ campaign at the Yonsei University in Seoul and at Taehwa Mountain sites are similar to Olympic Park even though most of the HCHO is locally produced by photochemistry, but has a relatively short lifetime of a few hours in polluted air where there is significant ozone and OH. However, at typical wind speeds of 10 -20 km/hour and a chemical lifetime of 2.5 hours (Dufour et al., 2009), HCHO can be transported about 25 – 50 km, which is far enough for some transport of HCHO between the PSI sites at Yonsei, Olympic Park, and Taewha Mtn. DC8 CAMS results over the Taehwa Mtn. site compared to PSI are given in Table 2 with differences similar to Olympic Park

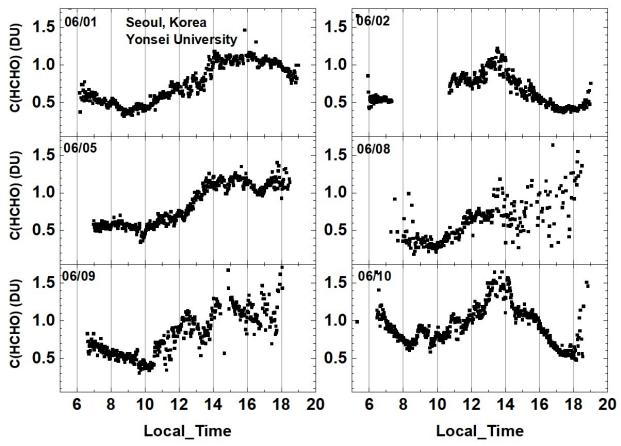


Fig. 17 Total column HCHO from Pandora Yonsei University, Seoul for 6 days in June 2016. C(HCHO) on 2 June 2016 has a peak value of 1.2 DU at 13:30 hours.

Table 2 Taehwa Mtn DC8 compared to PSI measurements (see 10 Jun in Fig. 18)

Date	LT	DC8 HCHO DU	PSI HCHO (DU)	Percent
11 May	08:25:19	0.4	0.6	67
18 May	08:34:26	0.4	0.5	80
30 May	12:05:00	0.5	0.9	56
10 Jun	08:22:45	1	1.16	86
10 Jun	12:22:53	1	1.5	67
10 Jun	15:46:03	1	1.3	77

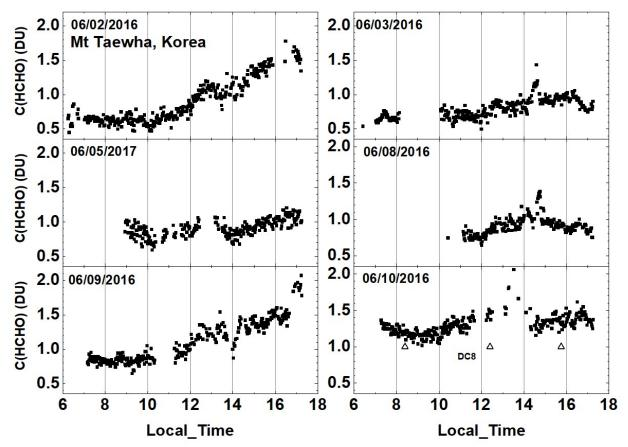


Fig. 18 Total column HCHO from Pandora at Taehwa Mountain for 6 days in June 2016. C(HCHO) on 2 June 2016 has a peak value of 1.7 DU at 16:20.  $\triangle$  are DC8 measurements on 10 June

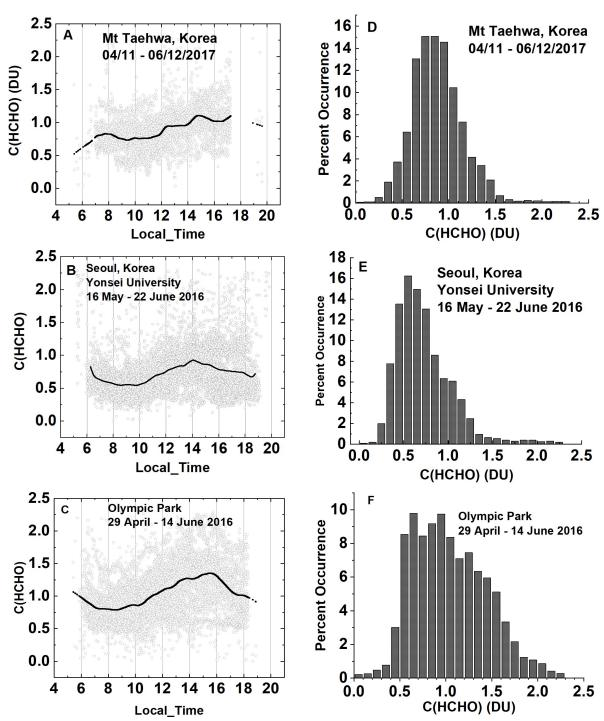


Fig. 19a Summary of total column HCHO for the stated dates during the KORUS-AQ campaign. The solid line is a Lowess(0.1) fit to the data. The sharp cutoffs in panel A, B, and C were caused obstructions of the direct sun from the PSI FOV in the afternoon.

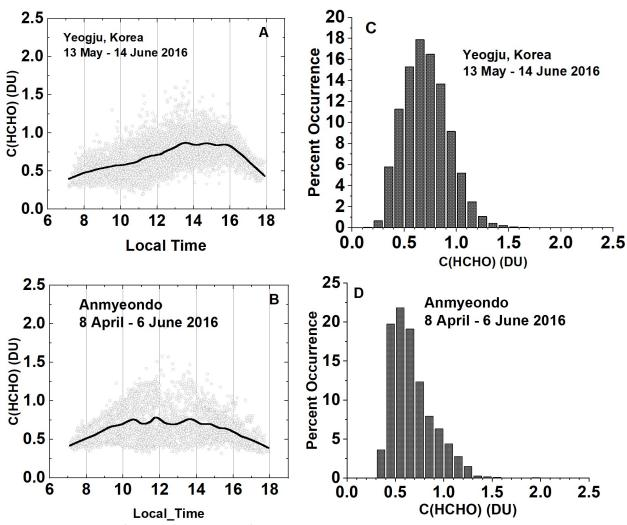


Fig. 19b Summary of total column HCHO for the stated dates during the KORUS-AQ campaign. Panels A and B represent the daily variation at a given local time. The solid line is a Lowess(0.1) fit to the data. Panels C and D show the frequency of occurrence (%) for different amounts of HCHO.

Figure 19a and 19b summarizes all of the C(HCHO) data obtained during KORUS-AQ at the five sites. The graphs on the left show all of the data points (light gray circles) as a function of the local time and a Lowess(0.1) fit to the data showing the average hourly behavior. The spread of the data about the Lowess(0.1) fit represents the day-to-day variation at a given local time. On average, Mt. Taehwa tends to increase throughout each day, while Yonsei and Olympic Park show maxima at 14:00 and 15:30, respectively. Similarly, in Fig. 18b Yeogju increases during the day having a maximum at 17:42 while Anmyeondo has a broad peak with maxima at 12:00 and 13:42.

The histograms on the right side of Fig. 19 represent the percent frequency of occurrence of C(HCHO) in 0.1 DU bins. C(HCHO) at Mt. Taehwa and Seoul rarely exceeds 1.5 DU

compared to Olympic Park where C(HCHO) > 2 DU for a significant fraction of time. The most frequent values are 0.6 DU for Seoul, 0.9 DU for Mt Taehwa, and over 1 DU for Olympic Park. Olympic Park also has a broader distribution towards higher values of C(HCHO) than other sites.

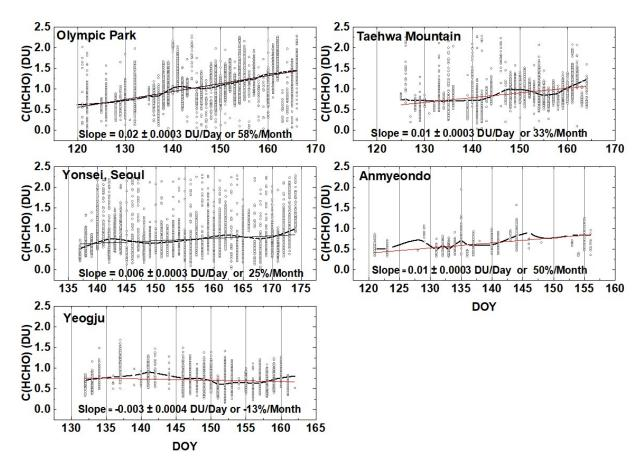


Fig. 20 The springtime change in C(HCHO) over about a 40 day period depending on the site. The "vertical bars" are the diurnal variation within each day of data. The thicker red curve is a Lowess(0.3) fit to the data, while the thin red line is a linear least squares fit. The Lowess(0.3) fit is approximately a 10-day local least-squares average.

The general intra-day C(HCHO) time dependence and C(HCHO) percent occurrence are shown for two additional sites (Fig. 19b), Yeogju and Amnyeondo. Yeogju shows an increase in C(HCHO) from morning to a peak value of 0.85 DU at 14:42, which then declines after 16:00. In contrast, Amnyeondo is almost symmetric with the sun position, having a maximum of about 0.77 DU near 12:00 and 13:42 hours.

The average change in C(HCHO) during the spring campaign at the five sites is summarized in Fig. 20. Of the sites, Olympic Park showed the largest change rate, 58 %/Month followed by Amnyeondo at 50 %/Month, then Taehwa (33 %/Month), Yonsei Seoul (25 %/Month), and Yeogju (-13 %/Month). Amnyeondo tends to have lower C(HCHO) amounts

because of its relatively isolated coastal location. These 2-month trends include seasonal increases during the campaign months May and June, 2016.

It is difficult to compare PSI C(HCHO) with OMI for the KORUS-AQ period, since OMI overpass C(HCHO) data for 2016 have some missing days (Fig. 21). For days with matching data points over Seoul, PSI C(HCHO) (approximately 0.8 DU) is almost always larger than the OMI values (0.2 DU) plus a few very high PSI values and two high OMI values. The general day-to-day variations are similar.

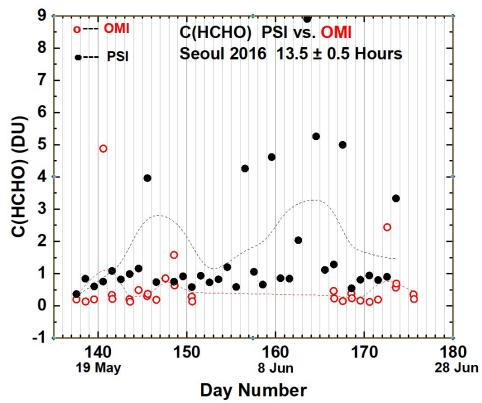


Fig. 21 Compare PSI ● and OMI o retrievals of C(HCHO) at 13.5 ± 0.5 hours. OMI overpass data, V03, are from https://avdc.gsfc.nasa.gov/index.php?site=1113974256&id=81

### 7 Summary

Nine Pandora Spectrometer Instruments, PSI, were installed at 8 sites in South Korea as part of the KORUS-AQ ground, aircraft, and satellite measurements for air-quality studies. The measurements made during the months of April to June by PSI showed that are very high amounts of urban pollution from NO<sub>2</sub> and HCHO, and more moderate, but still high values in Mt Taewha and Yeogju, which are some distance from the major urban centers,. An exceptional location was Amnyeondo, which is located on a west-coastal island adjacent to the Yellow Sea about 100 km south of Seoul. The urban areas show minimum values in the morning that rise rapidly throughout the day, peaking in the late afternoon for both C(NO<sub>2</sub>) and C(HCHO).

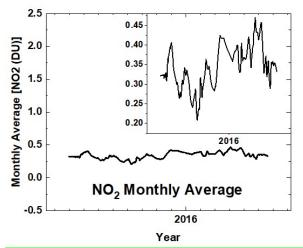
PSI direct-sun retrieved values of  $C(NO_2)$  and C(HCHO) are always larger than OMI retrieved  $C(NO_2)$  and C(HCHO) for the OMI overpass times (13.5  $\pm$  0.5 hours). In urban areas, PSI  $C(NO_2)$  averages are at least a factor of two larger than OMI averages. Similar differences are seen for C(HCHO) in Seoul. However, late afternoon values measured by PSI are even larger, implying that OMI measurements underestimate the effect of poor air quality on human health. The primary cause of the OMI underestimate is the large OMI FOV that includes regions containing low values of pollutants. In relatively clean areas, PSI and OMI are more closely in agreement.

PSI retrieved  $C(NO_2)$  amounts for Seoul frequently exceed 2 DU and occasionally reach 6 DU. Other urban centers in the south, Busan and Gwangju, have smaller  $C(NO_2)$  amounts, but exhibit a similar strong diurnal pattern, namely low values in the morning and high values later during midday. This behavior is expected because of the large number of urban automobiles and concentrated industry. Urban areas downwind from Seoul show high  $C(NO_2)$  amounts, but also show daily minimum amounts in the morning that increase later in the day. Two of the sites, Seoul and Busan, have long-term  $C(NO_2)$  data records, 2012 - 2016, that suggest a gradual decrease in  $C(NO_2)$  amounts in Korea. When compared with OMI, both ground-based PSI's and the 4STAR aircraft instrument onboard the DC8 show that the correlation is best for small values of  $C(NO_2)$ , most often seen in the troposphere and stratosphere and worst for high values that are usually in the boundary layer near their local sources. In Olympic Park, the measurements of significant values of C(HCHO) and high values of  $C(NO_2)$  in the afternoon suggest that there are increased boundary layer amounts of ozone.

C(HCHO) amounts were obtained for five sites, Yonsei University in Seoul, Olympic Park, Taehwa Mtn., Amnyeondo, and Yeoju. Of these the largest amounts of C(HCHO) were observed at Olympic Park, and Taehwa Mountain, both surrounded by significant amounts of vegetation. Comparisons of PSI results were made with overflights on the DC8 aircraft for Taehwa Mtn and Olympic Park showing a significant difference in total column HCHO. In all cases, PSI measured substantially more C(HCHO) than obtained from integrating the altitude profiles measured from the DC8 overflights.

## **Appendix**

Figure A1 illustrates the deseasonalization of the time series in Fig.6. The left panel reproduces the solid black curve in Fig. 6A or 6C in the inset. The right panel reproduces the solid curve in Fig. 6B and is magnified in the inset. The seasonal dependence in the left panel inset is almost non-existent in the right panel inset



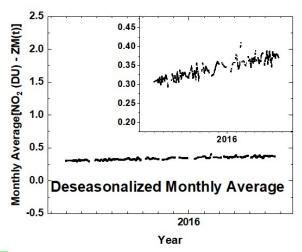


Fig. A1 An illustration of the deseasonalization (right panel) of the monthly running average of  $NO_2$  for the Gwangju site (left panel) shown in Fig. 6. The insets are magnifications of the main plots.

645	
646	
647	Data Sources
648	OMI Formaldehyde HCHO Version 03: <a href="https://avdc.gsfc.nasa.gov/index.php?site=1113974256&amp;id=81">https://avdc.gsfc.nasa.gov/index.php?site=1113974256&amp;id=81</a>
649	OMI Nitrogen Dioxide NO <sub>2</sub> Version 03 <a href="https://avdc.gsfc.nasa.gov/index.php?site=666843934&amp;id=13">https://avdc.gsfc.nasa.gov/index.php?site=666843934&amp;id=13</a>
650	Pandora KORUS-AQ https://avdc.gsfc.nasa.gov/pub/DSCOVR/Pandora/DATA/KORUS-AQ/
651	

652 **Author Contributions** 653 654 Jay Herman: Wrote most of the paper and performed the analysis and comparisons with the DC-8 655 aircraft measurements 656 Elena Spinei: Derived the formaldehyde altitude profiles suitable for comparison with Pandora data 657 Alan Fried: Obtained the HCHO profile data from the DC-8 CAMS instrument 658 Jhoon Kim: Provided support for the installation of Pandora instruments in Korea. 659 Jae Kim: Provided support for the Pandora located in Busan. 660 Woogyung Kim: Provided support in installing the Pandoras and analyzing the raw data 661 Alexander Cede: Provided calibration and data analysis support 662 Nader Abuhassan: Provided Pandora setup in Korea and provided the maintenance of calibration Michal Segal-Rozenhaimer: Provided the 4STAR NO<sub>2</sub> data from the DC-8 flights and the comparison with 663 Pandora 664 665 666 The authors declare that they have no conflict of interest.

#### 667 8 References

- Boersma, K. F., D. J. Jacob, M. Trainic, Y. Rudich, I. DeSmedt, R. Dirksen, and H. J. Eskes, Validation of
- 669 urban NO2 concentrations and their diurnal and seasonal variations observed from the SCIAMACHY and
- OMI sensors using in situ surface measurements in Israeli cities, Atmos. Chem. Phys., 9, 3867–3879,
- 671 2009.
- 672 Bernhard, G., C. R. Booth, and J. C. Ehramjian. Version 2 data of the National Science Foundation's
- 673 ultraviolet radiation monitoring network: South Pole. Journal of Geophysical Research (Atmospheres),
- 674 109(D21), 2004
- 675 Cede, Alexander, Manual for Blick Software Suite1.3 Version 7, 20 Apr 2017
- 676 https://avdc.gsfc.nasa.gov/pub/DSCOVR/Pandora/Documents/BlickSoftwareSuite\_Manual\_v7.pdf
- 677 Chimot, J., Vlemmix, T., Veefkind, J. P., de Haan, J. F., and Levelt, P. F.: Impact of aerosols on the OMI
- 678 tropospheric NO<sub>2</sub> retrievals over industrialized regions: how accurate is the aerosol correction of cloud-
- free scenes via a simple cloud model?, Atmos. Meas. Tech., 9, 359-382, https://doi.org/10.5194/amt-9-
- 680 359-2016, 2016.
- 681 Cleveland, William S., LOWESS: A program for smoothing scatterplots by robust locally weighted
- 682 regression. The American Statistician. **35** (1): 54. JSTOR 2683591. doi:10.2307/2683591, 1981.
- 683 684
- 684 Dufour, G., F. Wittrock, M. Camredon, M. Beekmann, A. Richter, B. Aumont, and J. P. Burrows,
- 685 SCIAMACHY formaldehyde observations: constraint for isoprene emission estimates over Europe?,
- 686 Atmos. Chem. Phys., 9, 1647–1664, 2009
- 687
- Dunagan, S. E., R. Johnson, J. Zavaleta, P. B. Russell, B. Schmid, C. Flynn, J. Redemann, Y. Shinozuka, J.
- 689 Livingston, and M. Segal-Rosenhaimer, 4STAR spectrometer for sky-scanning Sun-tracking atmospheric
- research: Instrument technology, Remote Sens. (Special Issue
- 691 "Optical Remote Sensing of the Atmosphere"), 5, 3872–3895, doi:10.3390/rs5083872, 2013.
- 692 Fried, A., Walega, J. G., Olson, J. R., Crawford, J. H., Chen, G., Weibring, P., ... Millet, D. B. (2008).
- 693 Formaldehyde over North America and the North Atlantic during the summer 2004 INTEX campaign:
- 694 Methods, observed distributions, and measurement-model comparisons. *Journal of Geophysical*
- 695 Research, 113(D10). https://doi.org/10.1029/2007JD009185, 2008.
- 696 Friedfeld, S., M. Fraser, K. Ensor, S. Tribble, D. Rehle, D. Leleux, F. Tittel Statistical analysis of primary and
- 697 secondary atmospheric formaldehyde, Atmospheric Environment, 36, 4767-4775, 2002.
- 698 Garcia, A.R., R. Volkamer, L.T. Molina, M.J. Molina, J. Samuelson, J. Mellqvist, B. Galle, S.C. Herndon, C.E.
- 699 Kolb, Separation of emitted and photochemical formaldehyde in Mexico City using a statistical analysis
- and a new pair of gas-phase tracers Atmospheric Chemistry Physics, 6, 4545-4557, 2006.
- 701 Goldberg D. et al., (2017), A High-Resolution And Observationally Constrained Omi NO2 Satellite
- 702 Retrieval, Atmos. Chem. Phys. Discuss., doi:10.5194/acp-2017-219, 2017.

- 703 Gueymard, Christian A., The sun's total and spectral irradiance for solar energy applications and solar
- radiation models. Solar energy, 76(4):423–453, 2004.
- Herman, Jay, Alexander Cede, Elena Spinei, George Mount, Maria Tzortziou, Nader Abuhassan, NO<sub>2</sub>
- 706 Column Amounts from Ground-based Pandora and MFDOAS Spectrometers using the Direct-Sun DOAS
- 707 Technique: Intercomparisons and Application to OMI Validation, J. Geophys. Res., 114, D13307,
- 708 doi:10.1029/2009JD011848, 2009.
- 709 Jung, Jinsang, JaeYong Lee, ByungMoon Kim, SangHyub Oh, Seasonal variations in the NO2 artifact from
- 710 chemiluminescence measurements with a molybdenum converter at a suburban site in Korea
- 711 (downwind of the Asian continental outflow) during 2015 2016, Atmospheric Environment 165, 290-
- 712 300, 2017.
- Kanaya, Y., Irie, H., Takashima, H., Iwabuchi, H., Akimoto, H., Sudo, K., Gu, M., Chong, J., Kim, Y. J., Lee,
- 714 H., Li, A., Si, F., Xu, J., Xie, P.-H., Liu, W.-Q., Dzhola, A., Postylyakov, O., Ivanov, V., Grechko, E.,
- 715 Terpugova, S., and Panchenko, M.: Long-term MAX-DOAS network observations of NO<sub>2</sub> in Russia and
- 716 Asia (MADRAS) during the period 2007–2012: instrumentation, elucidation of climatology, and
- 717 comparisons with OMI satellite observations and global model simulations, Atmos. Chem. Phys., 14,
- 718 7909-7927, https://doi.org/10.5194/acp-14-7909-2014, 2014.
- 719 Kim, Na Kyung, Yong Pyo Kim, Yu Morino, Jun-ichi Kurokawa, Toshimasa Ohara, Verification of NOx
- emission inventory over South Korea using sectoral activity data and satellite observation of NO<sub>2</sub> vertical
- 721 column densities, Atmospheric Environment, 77, 496-508, 2013.
- 722 Kim, Daewon, Hanlim Lee, Hyunkee Hong, Wonei Choi, Yun Gon Lee and Junsung Park, Estimation of
- 723 Surface NO2 Volume Mixing Ratio in Four Metropolitan Cities in Korea Using Multiple Regression Models
- 724 with OMI and AIRS Data, Remote Sens. 2017, 9, 627; doi:10.3390/rs9060627, 2017.
- 725 Krafta, Martin, Thomas Eikmannb, Andreas Kapposc, Nino Künzlid, Regula Rappe, Klaus Schneiderf,
- Heike Seitzb, Jens-Uwe Vossg, H.-Erich Wichmannh, he German view: Effects of nitrogen dioxide on
- human health derivation of health-related short-term and long-term values, International Journal of
- 728 Hygiene and Environmental Health, 208, 305–318, 2005.
- 729 Kramer, L.J., R. J. Leigh, J. J. Remedios, et al., "Comparison of OMI and Ground-Based in situ and
- 730 MAXDOAS Measurements of Tropospheric Nitrogen Dioxide in An Urban Area," J. Geophys. Res. 113,
- 731 D16S39, 2008.
- 732 Kurucz. Robert L., New atlases for solar flux, irradiance, central intensity, and limb intensity. Memorie
- 733 della Societa Astronomica Italiana Supplementi, 8:189, 2005.
- 734 Latza, Ute, , Silke Gerdes, and Xaver Baur, ffects of nitrogen dioxide on human health: Systematic review
- 735 of experimental and epidemiological studies conducted between 2002 and 2006, International Journal
- 736 of Hygiene and Environmental Health 212, Pages 271 287, doi.org/10.1016/j.ijheh.2008.06.003, 2009.

- 737 Lee, Greem, Hye-Ryun Oh, Chang-Hoi Ho, Jinwon Kim, Chang-Keun Song, Lim-Seok Chang, Jae-Bum Lee,
- 738 Seungmin Lee, Airborne Measurements of High Pollutant Concentration Events in the Free Troposphere
- over the West Coast of South Korea between 1997 and 2011, Aerosol and Air Quality Research, 16,
- 740 **1118–1130, 2016**.
- 741 Lei, W., Zavala, M., de Foy, B., Volkamer, R., Molina, M. J., and Molina, L. T.: Impact of primary
- 742 formaldehyde on air pollution in the Mexico City Metropolitan Area, Atmos. Chem. Phys., 9, 2607–2618,
- 743 2009.

758

761

- 744 Liteplo, R.G., R. Beauchamp, M.E. Meek, and R. Chénier. Formaldehyde. Geneva: International
- Programme on Chemical Safety; 2002. [18 May 2010]. (Concise International Chemical Assessment
- 746 Document 40) ( http://www.inchem.org/documents/cicads/cicads/cicad40.htm.
- 747 Luecken, D.J., W.T. Hutzell, M.L. Strum, G.A. Pouliot, Regional sources of atmospheric formaldehyde and
- acetaldehyde, and implications for atmospheric modeling, Atmospheric Environment 47, 477-490,
- 749 doi:10.1016/j.atmosenv.2011.10.005, 2012.
- 750 Meller, Richard, and Geert K Moortgat. Temperature dependence of the absorption cross sections of
- 751 formaldehyde between 223 and 323 k in the wavelength range 225-375 nm. Journal of Geophysical
- 752 Research: Atmospheres (19842012), 105(D6):70897101, 2000.
- Park. Junsung, Hanlim Lee, Jhoon Kim, Jay Herman, Woogyung Kim, Hyunkee Hong, Wonei Choi,
- 755 Jiwon Yang and Daewon Kim, HCHO column density retrieval using Pandora measurements in Seoul,
- Korea: Temporal characteristics and comparison with OMI measurement, Remote Sens., 10, 173;
- 757 doi:10.3390/rs10020173, 2018.
- Platt, U., D. Perner, and H. W. P¨atz, Simultaneous measurements of atmospheric CH2, O3 and NO2 by
- differential optical absorption, J. Geophys. Res. 84 (1979), 6329–6335, 1979.
- 762 Platt, U. Differential optical absorption spectroscopy (DOAS), Air monitoring by Spectroscopic Techiques
- 763 (M. Sigrist, ed.), John Wiley & Sons, Inc., 1994, pp. 27–84. [6] U. Platt, D. Perner, and H. W. P¨atz,
- 764 Simultaneous measurements of atmospheric CH2, O3 and NO2 by differential optical absorption, J.
- 765 Geophys. Res. 84 (1979), 6329–6335, 1994.
- 767 Richter D., P. Weibring, J. G. Walega, A. Fried, S. M. Spuler, M. S. Taubman: Compact highly sensitive
- 768 multi-species airborne mid-IR spectrometer, Appl. Phys. B, doi: 10.1007/s00340-015-6038-8, 2015.
- Russell, A. R., Perring, A. E., Valin, L. C., Bucsela, E. J., Browne, E. C., Wooldridge, P. J., and Cohen, R. C.: A
- high spatial resolution retrieval of NO2 column densities from OMI: method and evaluation, Atmos.
- 771 Chem. Phys., 11, 8543-8554, 2011.
- 772 Segal-Rosenheimer, M., P. B. Russell, B. Schmid, J. Redemann, J. M. Livingston, C. J. Flynn, R. R. Johnson,
- S. E. Dunagan, Y. Shinozuka1, J. Herman, A. Cede, N. Abuhassan, J. M. Comstock, J. M. Hubbe, A.
- 774 Zelenyuk3, and J. Wilson, (2014) Tracking elevated pollution layers with a newly developed

- 775 hyperspectral Sun/Sky spectrometer(4STAR): Results from the TCAP 2012 and 2013 campaigns, J.
- 776 Geophys. Res. Atmos., 119, 2611–2628, doi:10.1002/2013JD020884, 2014.
- 777 Shinozuka, Y., et al., Hyperspectral aerosol optical depths from TCAP flights, J. Geophys. Res. Atmos.,
- 778 118, 12,180–12,194, doi:10.1002/2013JD020596, 2013.
- 779 Spinei, E., N. Abuhassan, A Cede, M. Tiefengraber, M. Mueller, J. Herman, N. Nowak, B. Poche, S. Choi7,
- 780 A. Whitehill, J. Szykman, V. Lukas, D. Williams, R. Long, Jin Liao, Jason St. Clair, Glenn Wolfe, Thomas
- 781 Hanisco, Changmin Cho, Alan Fried, Petter Weibring, Dirk Richter, Robert Swap, James Walega, Pandora
- 782 formaldehyde measurements during KORUS-AQ over Olympic Park and Taehwa (South Korea, April-June
- 783 2016), (submitted to AMT), 2018.
- Thuillier, G., L. Floyd, T.N. Woods, R. Cebula, E. Hilsenrath, M. Hersé, and D. Labs. Solar irradiance
- reference spectra for two solar active levels. Advances in Space Research, 34(2):256–261, 2004.
- Vandaele, A.C., C. Hermans, P. C. Simon, M. Carleer, R. Colin, S. Fally, M. F. Mérienne, A. Jenouvrier, and
- 787 B. Coquart. Measurements of the NO2 absorption cross-section from 42,000 cm-1 to 10,000 cm-1 (238-
- 788 1000 nm) at 220 K and 294 K. Journal of Quantitative Spectroscopy and Radiative Transfer, 59: 171–184,
- 789 doi: 10.1016/S0022-4073(97)00168-4, 1998.
- 790 VanHoosier, Michael E. Solar ultraviolet spectral irradiance data with increased wavelength and
- 791 irradiance accuracy. InSPIE's 1996 International Symposium on Optical Science, Engineering, and
- 792 Instrumentation, pages 57–64. International Society for Optics and Photonics, 1996.
- 793 Walters, Wendell & Goodwin, Stanford & Michalski, Greg. (2015). The Nitrogen Stable Isotope
- 794 Composition ( $\delta$ 15N) of Vehicle Emitted NOx.. Environmental science & technology. 49.
- 795 10.1021/es505580v, 2015.
- 796 Zhang, Hongliang, Jingyi Li, Qi Ying, Birnur Buzcu Guven, and Eduardo P. Olaguer, Source apportionment
- of formaldehyde during TexAQS 2006 using a source-oriented chemical transport model, J. Geophys.
- 798 Res., 118, 1525–1535, doi:10.1002/jgrd.50197, 2013.
- 799 Zhu, Lei, Daniel J. Jacob, Frank N. Keutsch, Loretta J. Mickley, Richard Scheffe, Madeleine Strum, Gonzalo
- 800 González Abad, Kelly Chance, Kai Yang, Bernhard Rappenglück, Dylan B. Millet, Munkhbayar Baasandorj,
- 801 Lyatt Jaeglé, and Viral Shah, Formaldehyde (HCHO) As a Hazardous Air Pollutant: Mapping Surface Air
- 802 Concentrations from Satellite and Inferring Cancer Risks in the United States, Environmental Science &
- 803 Technology 51 (10), 5650-5657, DOI: 10.1021/acs.est.7b01356, 2017.

Acknowledgement

The author would like to thank the Pandora project for support in completing this study as well as
financial support from the KORUS-AQ project NNH15ZDA001N-KORUS. Dr. Jae Kim and Dr. Jhoon
Kim are supported by Korea Ministry of Environment as Public Technology Program based on
Environmental Policy (2017000160001). All data is available from a NASA data repository:
https://avdc.gsfc.nasa.gov/pub/DSCOVR/Pandora/DATA/KORUS-AQ/

https://avdc.gsfc.nasa.gov/pub/DSCOVR/Pandora/DATA/KORUS-AQ/

# 816 Tables

Table 1 KORUS-AQ Locations (South to North)				
Locations	Alt(m)	Latitude	Longitude	
Gwangju	33	35.2260N	126.8430W	
Busan	228	35.2353N	129.0825W	
Anmyeondo	41	36.5380N	126.3300W	
Taehwa Mtn	160	37.3123N	127.3106W	
Yeoju-1 & 2	90	37.3385N	127.4895W	
Songchon	49	37.4100N	127.5600W	
Olympic Park	26	37.5232N	127.1260W	
Seoul	181	37 5644N	126 9340W	

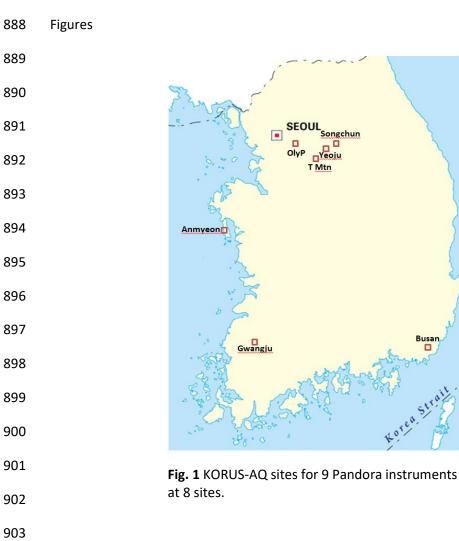
Table 2 Taehwa Mtn DC8 compared to PSI measurements in Fig. 18

Date	LT	DC8 HCHO DU	PSI HCHO	Percent
11 May	08:25:19	0.4	0.6	67
18 May	08:34:26	0.4	0.5	80
30 May	12:05:00	0.5	0.9	56
10 Jun	08:22:45	1	1.16	86
10 Jun	12:22:53	1	1.5	67
10 Jun	15:46:03	1	1.3	77

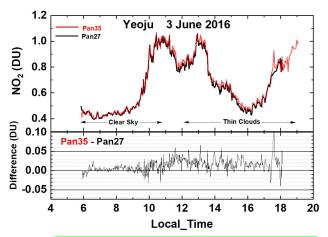
- 821 Figure Captions
- **Fig. 1** KORUS-AQ sites for 9 Pandora instruments at 8 sites.
- 823 Fig. 2a C(NO<sub>2</sub>) amounts from Pandora 27 and 35 in Yeoju, Korea during 3 June 2016 and their difference
- 824 | Pan35 Pan27 | < 0.05 DU.
- 825 Fig. 2b Pandora 35 estimate of cloud or aerosol reduced measured counts/second at approximately 500
- 826 nm
- Fig. 3. Frequency distributions of C(NO<sub>2</sub>) across the KORUS-AQ PSI network: April 20 to Jun 6 2016,
- 828 except as labelled. The axes vary for different sites.
- 829 Fig. 4 NO<sub>2</sub> time series vs day of the year (DOY) and diurnal variability (daily vertical extent) at 9 Pandora
- 830 sites. Notice the very high NO<sub>2</sub> amounts in Seoul and nearby Olympic Park. The black curves are
- aproximately weekly least squares running averages. Note: the vertical scales are different for each site
- to show the daily variability relative to the running average.
- Fig. 5 NO<sub>2</sub> amounts vs Day of the Year (DOY) and Local Time for six sites as labeled in each panel. Day
- 120=April 29, Day 130=May 9, Day 140=May 19, Day 150=May 29, Day 160=June 8, Day 170 =June 18.
  - Fig. 6 Approximately 1 year of daily column C(NO<sub>2</sub>) amount data (Panels A and D) and the monthly running average amount (dark plot in Pandels A and D). The data are from GIST at Gwangju and Amnyeondo. Panels A and D are the original time series with one data point every 80 seconds, panels B and E are the deseasonalized time series. Panels C and F are an expanded scale of the monthly running averages M(t) of C(NO<sub>2</sub>) that are identical to the solid lines in panels A and D. The vertical extent (panels A, B, D, and E) on a given day is the range of diurnal variation from early morning to late afternoon.
- 835 Fig. 7 (A) NO<sub>2</sub> time series at Yonsei University in Seoul NO<sub>2</sub>(grey) and (B) deseasonalized time series.
- Combined slope =  $-0.05 \pm 0.001$  DU/Year and Mean =  $1.2 \pm 0.8$  DU or the decrease is  $-4 \pm 0.08$  % / Year.
- 837 Seoul has no clear seasonal cycle.
- 838 Fig. 8 (A) Pusan University in Busan NO<sub>2</sub> daily time series (grey) and (B) deseasonalized time series with
- 839 linear trends.
- Fig. 9a Comparisons between the daily values of C(NO<sub>2</sub>) for OMI (black) and PSI (red) at Seoul and Busan
- for a 5-year period. Solid lines show the average seasonal variation (Lowess(0.1)), see also Fig. 9b. Linear
- interpolation is used where there are missing data points.
- 843 Fig. 9b Comparisons between the seasonal averages for C(NO<sub>2</sub>) from OMI (black) and PSI (red) at Seoul
- and Busan for a 5-year period. The lower panels show the seasonal difference between the PSI and
- 845 OMI. The individual data points are shown derived from a Lowess(0.1) smoothing, approximately a 3-
- month running averages of the daily data. Interpolation has been used where there are missing data
- 847 points.

- 848 Fig. 10 C(NO₂) time series from Pandora (red) and OMI (black) for GIST University in Gwangju Korea and
- their differences. The comparison is formed from time coincidences between Pandora and OMI.
- Fig. 11 A correlation plot of C(NO<sub>2</sub>) from 4STAR onboard the DC-8 compared to the C(NO<sub>2</sub>) amount
- measured by the PSI at Olympic Park on nine different days. The solid black line is the 1:1 line drawn for
- reference. The dashed line represents the data linear fit, with a slope of 1.05, and a correlation
- 853 coefficient  $r^2 = 0.7$ , as shown on the plot.
- 854 Fig. 12 C(HCHO) from PSI at Olympic Park for 6 days in June 2016. C(HCHO) on 2 June 2016 has a peak
- 855 value of 2.3 DU at 14:30 hours.
- 856 Fig. 13 Pandora measured formaldehyde amounts vs day of the year and local time for 29 April 2016 to
- 857 11 June 2016 in Olympic Park.
- Fig. 14 HCHO altitude profile measured onboard the DC8 on 4 May at 07:54 (A) and 11:54 (B) local time
- over Olympic Park, Korea. Panel C: PSI measurements of total column HCHO. Vertical bars mark the DC8
- 860 flight duration for the profiles yielding altitude integrated column amounts of 0.38 and 0.26 DU.
- Fig. 15 DC-8 HCHO measurements over Olympic Park on June 4. The continuous blue profiles
- show the 1-second HCHO data while the black points with error bars show the 10-second
- average and standard deviation of this data at points of closest approach above the Olympic
- 864 Park site.
- 865 Fig. 16 HCHO altitude profile measured onboard the DC8 on 5 June at 8:30 (A) and 15:21 (B) local time
- over Olympic Park, Korea. Panel C: PSI measurements of total column HCHO. Vertical bars mark the DC8
- 867 flight duration for the profiles yielding column amounts of 0.60 and 0.82 DU.
- 868 Fig. 17 Total column HCHO from Pandora Yonsei University, Seoul for 6 days in June 2016. HCHO on 2
- 869 June 2016 has a peak value of 1.2 DU at 13:30 hours.
- 870 Fig. 18 Total column HCHO from Pandora Taehwa Mountain for 6 days in June 2016. HCHO on 2 June
- 871 2016 has a peak value of 1.2 DU at 12:45. Δ are DC8 measurements on 10 June.
- Fig. 19a Summary of total column HCHO for the stated dates during the KORUS-AQ campaign. The solid
- 873 line is a Lowess(0.1) fit to the data. The sharp cutoffs in panel A, B, and C were caused obstructions of
- the direct sun from the PSI FOV in the afternoon.
- 875 Fig. 19b Summary of total column HCHO for the stated dates during the KORUS-AQ campaign. Panels A
- and B represent the daily variation at a given local time. The solid line is a Lowess(0.1) fit to the data.
- Panels C and D show the frequency of occurrence (%) for different amounts of HCHO.
- Fig. 20 The springtime change in C(HCHO) over about a 40 day period depending on the site.
- The "vertical bars" are the diurnal variation within each day of data. The thicker red curve is a
- Lowess(0.3) fit to the data, while the thin red line is a linear least squares fit. The Lowess(0.3) fit
- is approximately a 10-day local least-squares average.

882	Fig. 21 Compare PSI ● and OMI o retrievals of C(HCHO) at 13.5 ± 0.5 hours. OMI overpass data, V03, are
883	from <a href="https://avdc.gsfc.nasa.gov/index.php?site=1113974256&amp;id=81">https://avdc.gsfc.nasa.gov/index.php?site=1113974256&amp;id=81</a>
884	Fig. A1 An illustration of the deseasonalization (right panel) of the monthly running average of NO <sub>2</sub> for
885	the Gwangju site (left panel) shown in Fig. 6. The insets are magnifications of the main plots.
886	
887	



F01



1.6 Yeoju 3 June 2016 1.4 1.2 Counts/sec x 10<sup>7</sup> 1.0 8.0 0.6 0.4 0.2 0.0 -0.2 8 10 12 14 16 20 18 **Local Time** 

Fig. 2a  $C(NO_2)$  amounts from Pandora 27 and 35 in Yeoju, Korea during 3 June 2016 and their difference |Pan35 - Pan27| < 0.05 DU.

Fig. 2b Pandora 35 estimate of cloud or aerosol reduced measured counts/second at approximately 500 nm.

F02

909

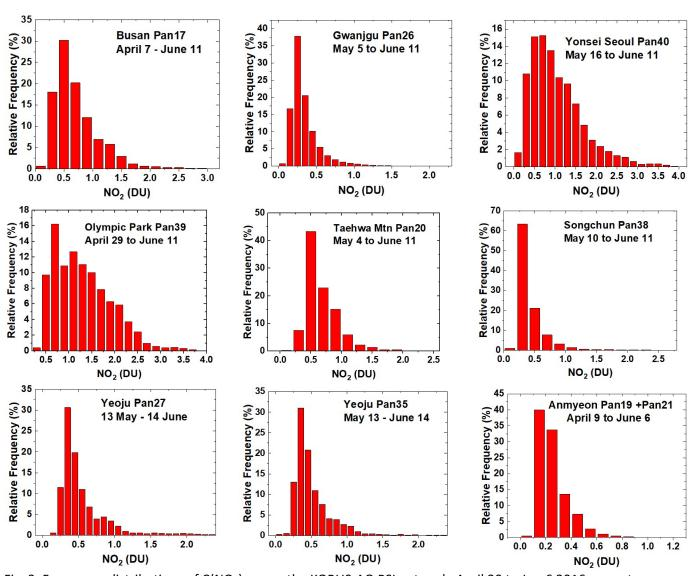


Fig. 3. Frequency distributions of  $C(NO_2)$  across the KORUS-AQ PSI network: April 20 to Jun 6 2016, except as labelled. The axes vary for different sites.

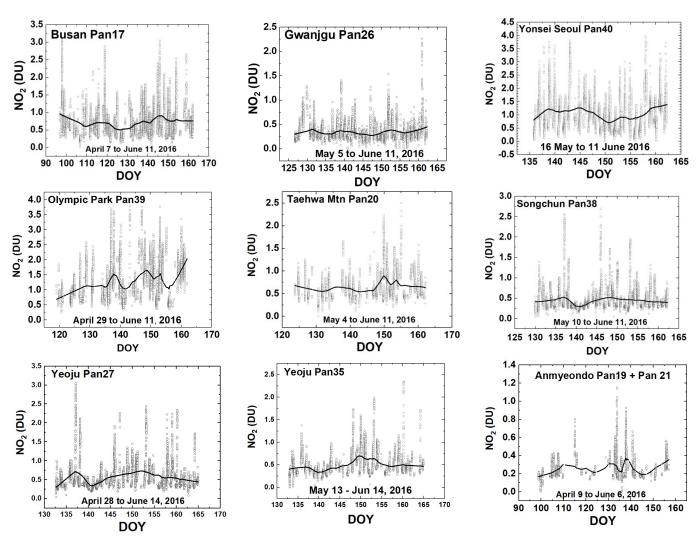


Fig. 4  $NO_2$  time series vs day of the year (DOY) and diurnal variability (daily vertical extent) at 9 Pandora sites. Notice the very high  $NO_2$  amounts in Seoul and nearby Olympic Park. The black curves are aproximately weekly least squares running averages. The daily vertical extent corresponds to diurnal variation (Fig. 2). Note: the vertical scales are different for each site to show the daily variability relative to the running average.

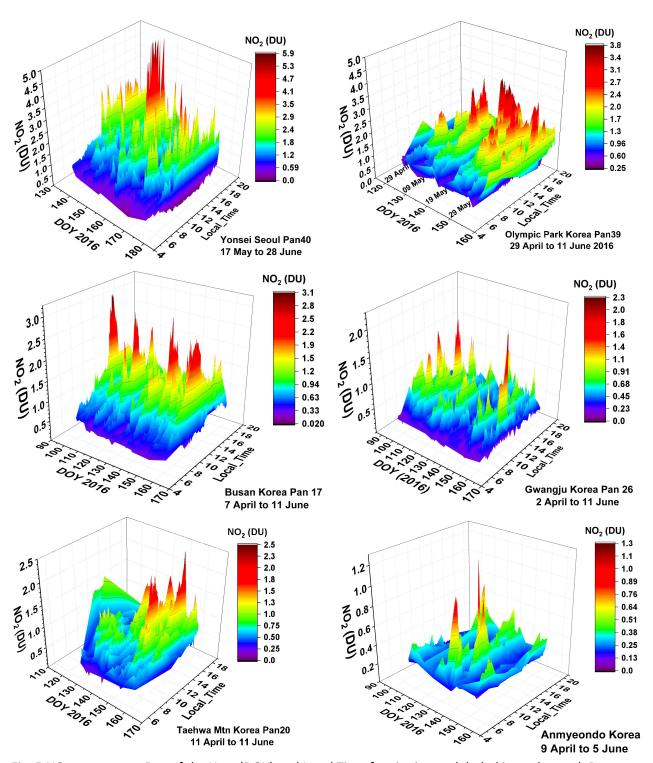


Fig. 5  $NO_2$  amounts vs Day of the Year (DOY) and Local Time for six sites as labeled in each panel. Day 120=April 29, Day 130=May 9, Day 140=May 19, Day 150=May 29, Day 160=June 8, Day 170 =June18.

916

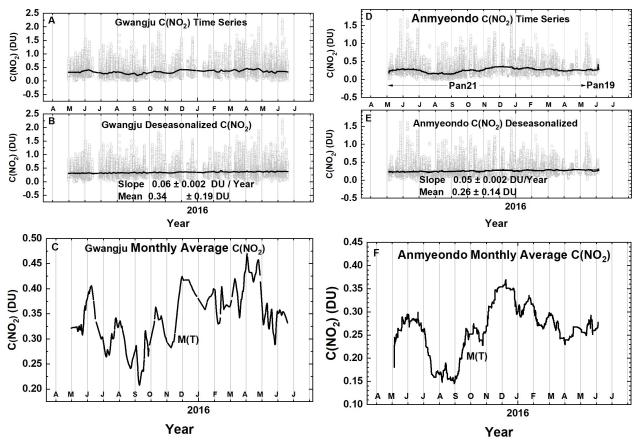


Fig. 6 Approximately 1 year of daily column  $C(NO_2)$  amount data (Panels A and D) and the monthly running average amount (dark plot in Pandels A and D). The data are from GIST at Gwangju and Amnyeondo. Panels A and D are the original time series with one data point every 80 seconds, panels B and E are the deseasonalized time series. Panels C and F are an expanded scale of the monthly running averages M(t) of  $C(NO_2)$  that are identical to the solid lines in panels A and D. The vertical extent (panels A, B, D, and E) on a given day is the range of diurnal variation from early morning to late afternoon.

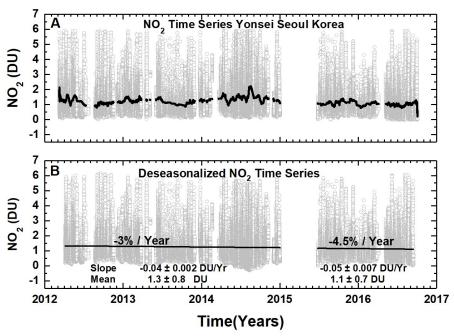


Fig. 7 (A)  $NO_2$  time series at Yonsei University in Seoul  $NO_2$ (grey) and (B) deseasonalized time series. Combined slope =  $-0.05 \pm 0.001$  DU/Year and Mean =  $1.2 \pm 0.8$  DU or the decrease is  $-4 \pm 0.08$  % / Year. Seoul has no clear seasonal cycle.

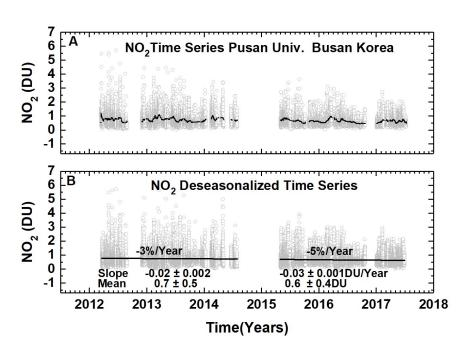


Fig. 8 (A) Pusan University in Busan  $NO_2$  daily time series (grey) and (B) deseasonalized time series with linear trends.

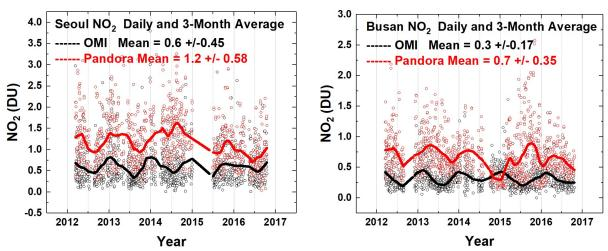


Fig. 9a Comparisons between the daily values of C(NO<sub>2</sub>) for OMI (black) and PSI (red) at Seoul and Busan for a 5-year period. Solid lines show the average seasonal variation (Lowess(0.1)), see also Fig. 9b. Linear interpolation is used where there are missing data points.

F09a

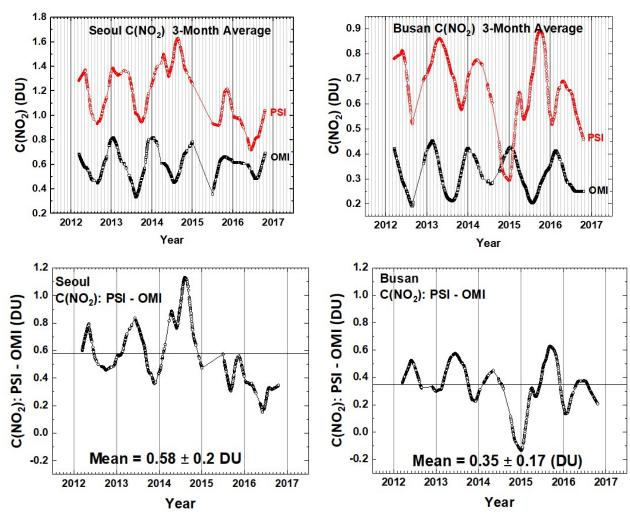


Fig. 9b Comparisons between the seasonal averages for  $C(NO_2)$  from OMI (black) and PSI (red) at Seoul and Busan for a 5-year period. The lower panels show the seasonal difference between the PSI and OMI. The individual data points are shown derived from a Lowess(0.1) smoothing, approximately a 3-month running averages of the daily data. Interpolation has been used where there are missing data points.

F09b

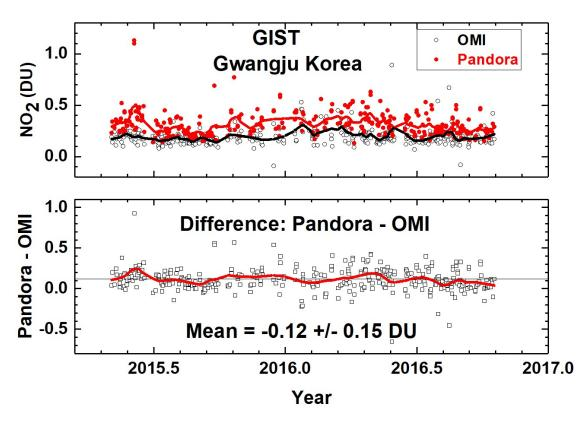


Fig. 10 C(NO<sub>2</sub>) time series from Pandora (red) and OMI (black) for GIST University in Gwangju Korea and their differences. The comparison is formed from time coincidences between Pandora and OMI.

**F10** 

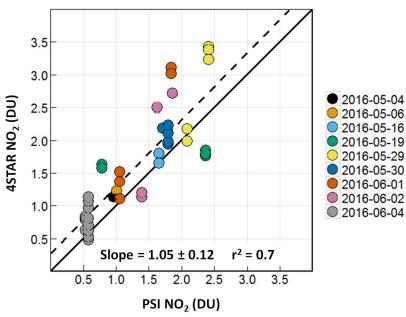


Fig. 11 A correlation plot of  $C(NO_2)$  from 4STAR onboard the DC-8 compared to the  $C(NO_2)$  amount measured by the PSI at Olympic Park on nine different days. The solid black line is the 1:1 line drawn for reference. The dashed line represents the data linear fit, with a slope of 1.05, and a correlation coefficient  $r^2 = 0.7$ , as shown on the plot.

**F11** 

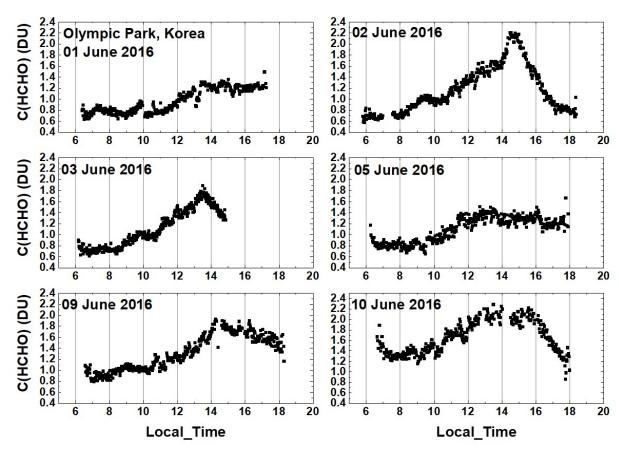


Fig. 12 C(HCHO) from PSI at Olympic Park for 6 days in June 2016. C(HCHO) on 2 June 2016 has a peak value of 2.3 DU at 14:30 hours.

**F12** 

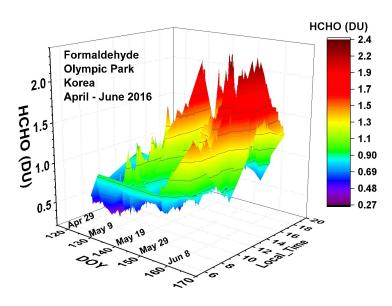
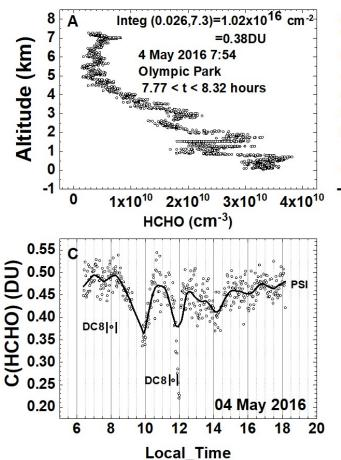


Fig. 13 Pandora measured formaldehyde amounts vs day of the year and local time for 29 April 2016 to 11 June 2016 in Olympic Park.

**F13** 



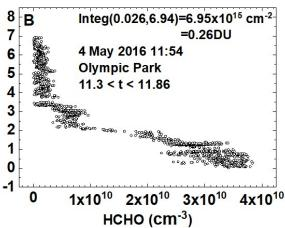


Fig. 14 HCHO altitude profile measured onboard the DC8 on 4 May at 07:54 (A) and 11:54 (B) local time over Olympic Park, Korea. Panel C: PSI measurements of total column HCHO. Vertical bars mark the DC8 flight duration for the profiles yielding altitude integrated column amounts of 0.38 and 0.26 DU.

F14

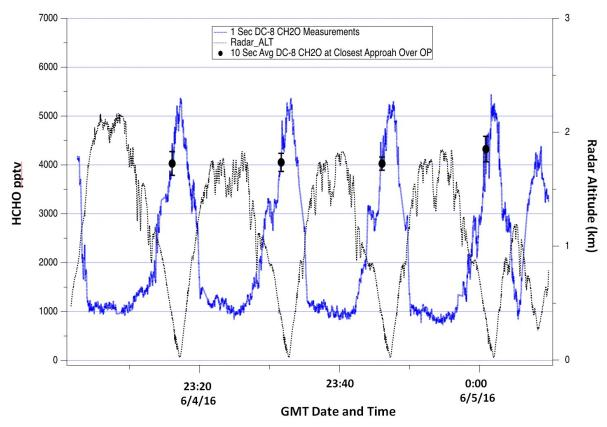
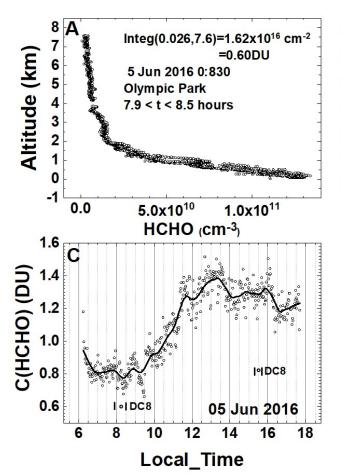


Fig. 15 DC-8 HCHO measurements over Olympic Park on June 4. The continuous blue profiles show the 1-second HCHO data while the black points with error bars show the 10-second average and standard deviation of this data at points of closest approach above the Olympic Park site.

**F15** 



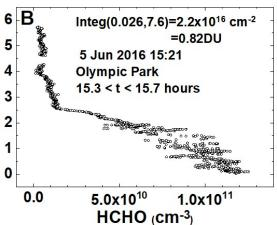


Fig. 16 HCHO altitude profile measured onboard the DC8 on 5 June at 8:30 (A) and 15:21 (B) local time over Olympic Park, Korea. Panel C: PSI measurements of total column HCHO. Vertical bars mark the DC8 flight duration for the profiles yielding column amounts of 0.60 and 0.82 DU.

F16



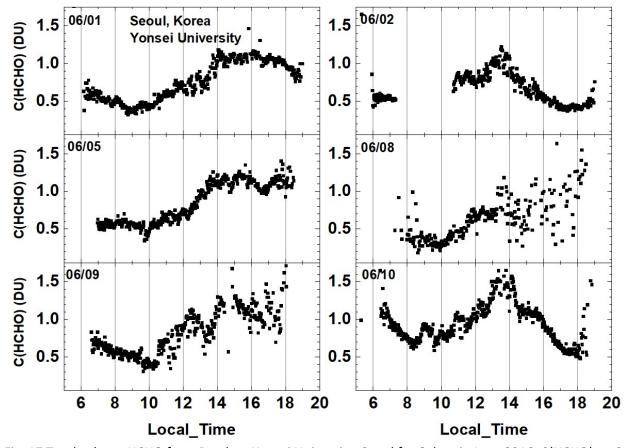


Fig. 17 Total column HCHO from Pandora Yonsei University, Seoul for 6 days in June 2016. C(HCHO) on 2 June 2016 has a peak value of 1.2 DU at 13:30 hours.

## **F17**

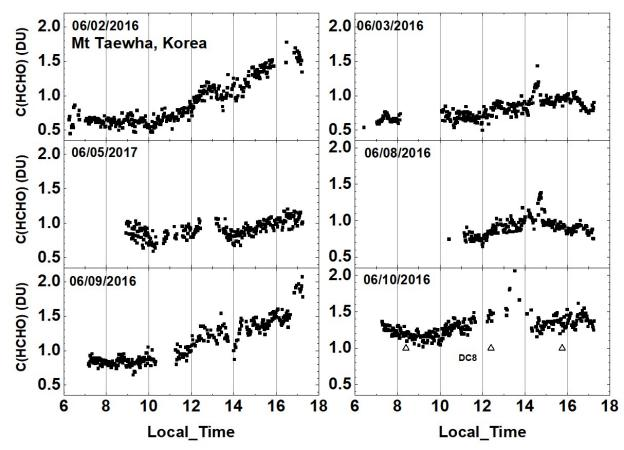


Fig. 18 Total column HCHO from Pandora at Taehwa Mountain for 6 days in June 2016. C(HCHO) on 2 June 2016 has a peak value of 1.7 DU at 16:20.  $\triangle$  are DC8 measurements on 10 June

**F18** 

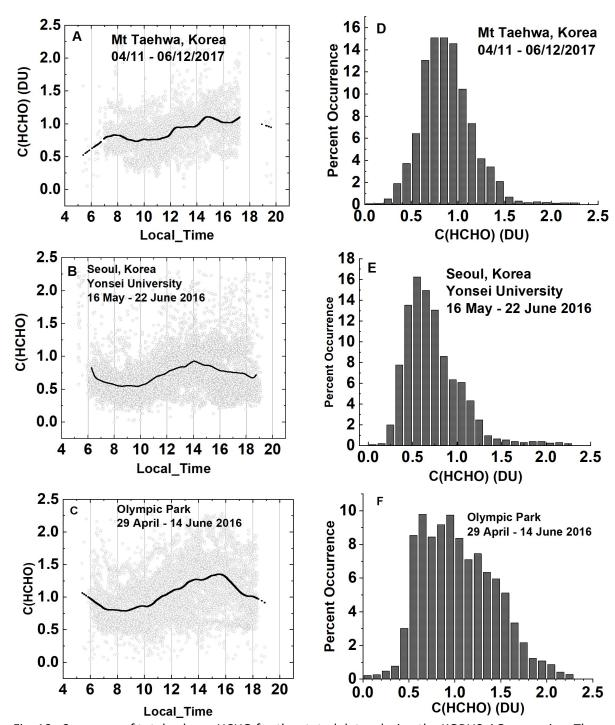


Fig. 19a Summary of total column HCHO for the stated dates during the KORUS-AQ campaign. The solid line is a Lowess(0.1) fit to the data. The sharp cutoffs in panel A, B, and C were caused obstructions of the direct sun from the PSI FOV in the afternoon.

F19a

963

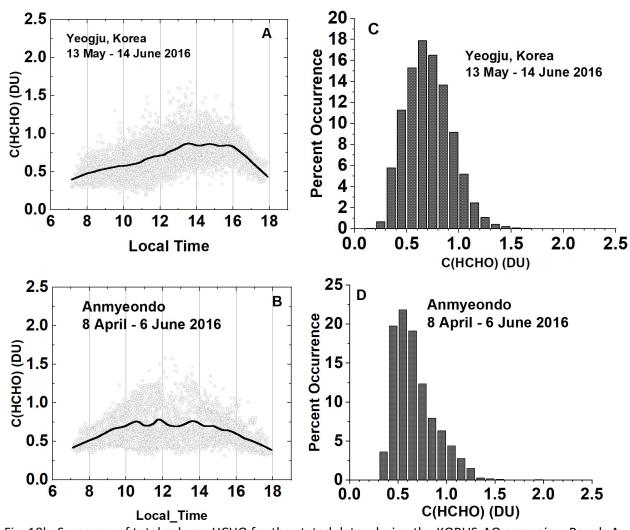


Fig. 19b Summary of total column HCHO for the stated dates during the KORUS-AQ campaign. Panels A and B represent the daily variation at a given local time. The solid line is a Lowess(0.1) fit to the data. Panels C and D show the frequency of occurrence (%) for different amounts of HCHO.

**F19b** 

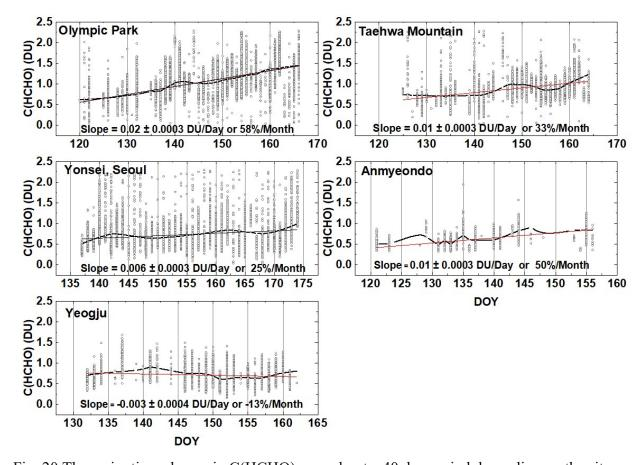


Fig. 20 The springtime change in C(HCHO) over about a 40 day period depending on the site. The "vertical bars" are the diurnal variation within each day of data. The thicker red curve is a Lowess(0.3) fit to the data, while the thin red line is a linear least squares fit. The Lowess(0.3) fit is approximately a 10-day local least-squares average.

**F20** 

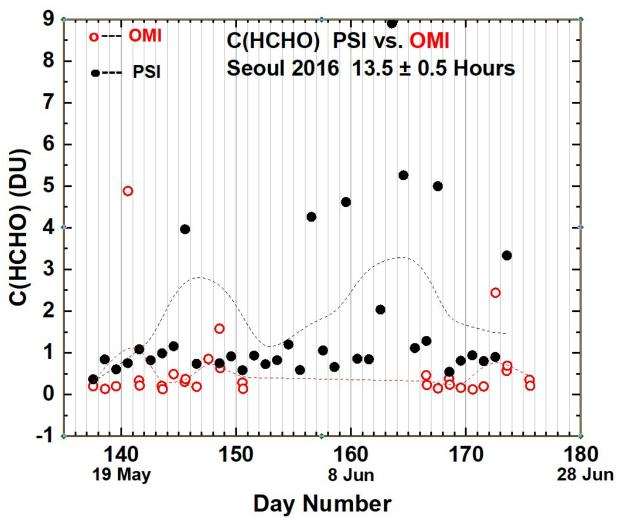


Fig. 21 Compare PSI ● and OMI o retrievals of C(HCHO) at 13.5 ± 0.5 hours. OMI overpass data, V03, are from https://avdc.gsfc.nasa.gov/index.php?site=1113974256&id=81

**F21** 

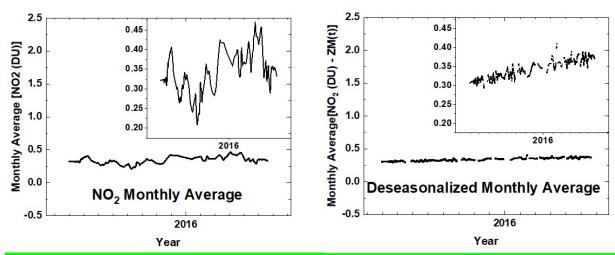


Fig. A1 An illustration of the deseasonalization (right panel) of the monthly running average of  $NO_2$  (left panel) shown in Fig. 6. The insets are magnifications of the main plots.

FA1